

Synthesis of ultra-refractory transition metal diboride compounds

Fahrenholtz, William G.; Binner, Jon; Zou, Ji

DOI:
[10.1557/jmr.2016.210](https://doi.org/10.1557/jmr.2016.210)

Document Version
Peer reviewed version

Citation for published version (Harvard):
Fahrenholtz, WG, Binner, J & Zou, J 2016, 'Synthesis of ultra-refractory transition metal diboride compounds', *Journal of Materials Research*, vol. 31, no. 18, pp. 2757-2772. <https://doi.org/10.1557/jmr.2016.210>

[Link to publication on Research at Birmingham portal](#)

Publisher Rights Statement:
Checked for eligibility: 04/10/2016.

COPYRIGHT: © Materials Research Society 2016

Fahrenholtz, W.G., Binner, J. and Zou, J. (2016) 'Synthesis of ultra-refractory transition metal diboride compounds', *Journal of Materials Research*, 31(18), pp. 2757–2772. doi: 10.1557/jmr.2016.210.

<https://www.cambridge.org/core/journals/journal-of-materials-research/article/synthesis-of-ultra-refractory-transition-metal-diboride-compounds/439AC30524D1F1E2970F306B038DD857>

General rights

Unless a licence is specified above, all rights (including copyright and moral rights) in this document are retained by the authors and/or the copyright holders. The express permission of the copyright holder must be obtained for any use of this material other than for purposes permitted by law.

- Users may freely distribute the URL that is used to identify this publication.
- Users may download and/or print one copy of the publication from the University of Birmingham research portal for the purpose of private study or non-commercial research.
- User may use extracts from the document in line with the concept of 'fair dealing' under the Copyright, Designs and Patents Act 1988 (?)
- Users may not further distribute the material nor use it for the purposes of commercial gain.

Where a licence is displayed above, please note the terms and conditions of the licence govern your use of this document.

When citing, please reference the published version.

Take down policy

While the University of Birmingham exercises care and attention in making items available there are rare occasions when an item has been uploaded in error or has been deemed to be commercially or otherwise sensitive.

If you believe that this is the case for this document, please contact UBIRA@lists.bham.ac.uk providing details and we will remove access to the work immediately and investigate.

Synthesis of Ultra-Refractory Transition Metal Diboride Compounds

William G. Fahrenholtz

Missouri University of Science and Technology, Rolla, MO United States 65409

Jon Binner and Ji Zou

University of Birmingham, Edgbaston, Birmingham, B15 2TT, United Kingdom

Abstract

This paper critically evaluates methods used to synthesize boride compounds with emphasis on diborides of the early transition metals. The earliest reports of the synthesis of boride ceramics used impure elemental powders to produce multi-phase reaction products; phase-pure borides were only synthesized after processes were established to purify elemental boron. Carbothermal reduction of the corresponding transition metal oxides emerged as a viable production route and continues to be the primary method for synthesis of commercial transition metal diboride powders. Even though reaction-based processes and chemical synthesis methods are mainly used for research studies, they are powerful tools for producing diborides because they provide the ability to tailor purity and particle size. The choice of synthesis method requires balancing factors that include cost, purity, and particle size with the performance needed in expected applications.

Corresponding Author

William G. Fahrenholtz

Missouri University of Science and Technology, Rolla, MO United States 65409

billf@mst.edu

Keywords

Boron, compound, ceramic

Synthesis of Ultra-Refractory Transition Metal Diboride Compounds

William G. Fahrenholtz^a, Jon Binner^b, and Ji Zou^b

^a Missouri University of Science and Technology, Rolla, MO United States

^b University of Birmingham, Birmingham, United Kingdom

Abstract

This paper critically evaluates methods used to synthesize boride compounds with emphasis on diborides of the early transition metals. The earliest reports of the synthesis of boride ceramics used impure elemental powders to produce multi-phase reaction products; phase-pure borides were only synthesized after processes were established to purify elemental boron. Carbothermal reduction of the corresponding transition metal oxides emerged as a viable production route and continues to be the primary method for synthesis of commercial transition metal diboride powders. Even though reaction-based processes and chemical synthesis methods are mainly used for research studies, they are powerful tools for producing diborides because they provide the ability to tailor purity and particle size. The choice of synthesis method requires balancing factors that include cost, purity, and particle size with the performance needed in expected applications.

I. Introduction

Transition metals (TMs) form a tremendous variety of boride compounds ranging from boron-rich dodecahedron or icosahedral structures such as ScB_{12} and YB_{25} to metal-rich close-packed compounds such as W_2B_5 and TiB . From the larger family of boride compounds, the early transition metals all form metal-rich refractory borides TMs, Table I,¹²¹ although synthesis methods described herein are applicable to other boride compounds with different stoichiometries and structures, including ternary borides. From the larger family of metal-rich

TM borides, the paper focuses on methods to produce Ti, Zr, and Hf diborides, which share the AlB_2 structure with other TM diborides including CrB_2 , TaB_2 , and NbB_2 . The TM diborides have a complex mix of bond types resulting in a remarkable combination of metal-like and ceramic-like properties.²²⁻²⁵ The AlB_2 structure consists of layers of close-packed metal atoms that alternate with boron in graphite-like sheets. Metallic bonding in the TM layers leads to high electrical (10^7 S/m for ZrB_2)^{26,27} and thermal (~ 130 W/m \cdot K for ZrB_2)²⁷⁻²⁹ conductivities, while strong covalent bonding in the B layers gives high hardness (~ 33 GPa for TiB_2)³⁰ and elastic modulus (~ 560 GPa for TiB_2)³¹ values. Strong cohesion between TM and B layers is the result of complex bonding that includes ionic, hybridized covalent, and metallic character.^{32,33} The same characteristics (high melting temperature, strong covalent bonds) that give TM boride compounds attractive properties also result in challenges related to producing high purity ceramics with high relative density.³⁴ Based on their inherent properties, TM diboride compounds have the potential to withstand extreme environments such as those associated with hypersonic aerospace vehicles, rocket motors, scramjet engines, lightweight armor, high speed cutting tools, refractories for molten metal contact applications, plasma-facing materials for nuclear fusion reactors, and fuel forms for advanced nuclear fission reactors.³⁵⁻⁴⁶ These applications involve temperatures, heat fluxes, radiation levels, strain rates, and/or chemical reactivities that are beyond the capabilities of existing structural materials.⁴⁷ For example, the sharp leading edges of hypersonic aerospace vehicles are expected to experience temperatures of 2000°C or higher and heat fluxes of more than 300 W/cm²,⁴⁸⁻⁵⁰ which are well beyond the capabilities of the current generations of Si-based structural ceramics and Ni-based superalloys. Realization of improved boron-based ceramics could enable revolutionary advances in these and other

technologies leading to broad improvements in performance, operating lifetime, and/or efficiency.

Existing and future boron-based ceramics will find application in forms ranging from thin films to bulk structures.⁵¹ Accordingly, different synthesis methods will best suit the different structures. For example, hard boride coatings for high speed cutting tools might best be synthesized and deposited by vapor phase methods,⁵² whereas liquid precursors would be preferred to produce ceramic matrices for continuous-fiber reinforced composites.⁵³ Other high temperature structural applications will require fabrication of bulk ceramics, which might be best accomplished by processes that combine reactive synthesis with densification.⁵⁴ Hence, a variety of methods are needed, some of which will only be capable of producing milligrams of material per day whereas others could produce kilograms of high purity ceramic powders.

The purpose of this paper is to review and evaluate methods used to synthesize TM diboride compounds. The focus is on refractory diborides of early transition metals, but the same methods can be used to produce new boron-based ceramics with compositions, microstructures, and/or properties tailored for future applications.

II. Historic Reports

Synthesis processes for TM diborides trace back to the late 1800s and early 1900s. Henri Moissan identified a number of boride compounds,^{55,56} including mentioning titanium boride in a study of the purification of titanium metal reported in 1895,⁵⁷ as part of his pioneering work using the electric arc furnace to produce compounds by fusion processes. In 1901, Tucker and Moody described the synthesis of zirconium boride by reaction of elements, although they assigned the formula Zr_3B_4 to their impure material.^{58,59} Likewise, Wedekind prepared impure borides by vacuum melting.⁶⁰ One of the first reports of carbothermal reduction, Reaction 1

shown in Table II, to produce diborides was by McKenna who produced TiB_2 and ZrB_2 in 1936.⁶¹ In contrast to the earlier papers on most other TM diborides, the first report of the synthesis of HfB_2 was in 1931.⁶² Hafnium itself was not isolated until 1923,⁶³ which accounts for the delay in describing synthesis of HfB_2 compared to other TM borides. While TM boride compounds were reported in this era, none of the materials were phase pure.

Preparation of phase pure diborides was enabled by Kiessling's production of high purity boron in the late 1940s.⁶⁴ This breakthrough led to the synthesis of a number of nominally pure TM diboride compounds,⁶⁵⁻⁶⁷ including zirconium diboride,⁶⁸ by reaction of boron with elemental metals, Reaction 2, as well as later work on borothermal reduction of oxides, Reaction 3.⁶⁹⁻⁷³ Other methods such as reactions with boron carbide, Reactions 4 and 5,⁷⁴⁻⁷⁶ metallothermic reduction, Reactions 6 and 7,^{77,78} electrolysis of fused salts, Reaction 8,^{79,80} and vapor phase methods, Reaction 9⁸¹⁻⁸³ were also used to produce boride compounds. Through the 1950s and 1960s, research on diborides, particularly those of Ti, Zr and Hf, typically utilized commercially available powders.⁸⁴⁻⁸⁶ Some of the exceptions were the phase equilibria studies by Rudy⁸⁷ and the examination of borides of alkali,⁸⁸ alkaline earth,⁸⁹ rare-earth,⁹⁰ or less-common transition metals⁹¹ as well as studies of ternary and higher borides.^{92,93} This trend continues to hold true to the present time whereby the majority of studies of the more common diborides (e.g., TiB_2 , ZrB_2 , and HfB_2) use commercial powders whereas self-synthesis is mainly used for other borides.

III. Reduction Processes

Commercially available TM diboride powders are predominantly synthesized by carbothermal reduction of the corresponding TM oxides, Reaction 1.⁹⁴⁻⁹⁸ The resulting powders typically contain oxygen and excess carbon as impurities along with any metallic impurities

present in the starting raw materials. For example, commercial ZrB₂ is produced from naturally-occurring zircon ores, which contain Hf as an impurity. Therefore, most commercial ZrB₂ powders contain Hf. A recent analysis showed that a widely used commercial powder (H.C. Starck, Grade B) contained ~1.7 wt.% Hf,⁹⁹ although the natural abundance of Hf in Zr-bearing minerals generally ranges from 1 to 5 wt% depending on the deposit.¹⁰⁰ While the Hf impurities do not appear to have an affect on most properties, recent reports have shown that the presence of Hf has a strong, negative impact on thermal transport with thermal conductivity decreasing from ~140 W/m•K for ZrB₂ with a Hf content of 0.01 at% to ~100 W/m•K for ZrB₂ with the natural abundance of Hf (0.33 at%).¹⁰¹ Likewise, the natural Hf content of ZrB₂ reduces its heat capacity by about 15% compared to powders synthesized from Zr with lower Hf contents.¹⁰²

Carbothermal reduction of transition metal oxides by Reaction 1 only becomes thermodynamically favorable at elevated temperatures. For example, the standard state change in Gibbs' free energy ($\Delta G_{\text{rxn}}^{\circ}$) for the formation of ZrB₂ by carbothermal reduction, Reaction 10, is given by Equation 11, which shows that the reaction becomes favorable (i.e., $\Delta G_{\text{rxn}}^{\circ}$ is less than zero) above ~1500°C. In addition, carbothermal reduction reactions are highly endothermic ($\Delta H_{\text{rxn}}^{\circ} = 1475$ kJ at 298 K). As a result of these factors, carbothermal reduction reactions are carried out at elevated temperatures.



$$\Delta G_{\text{rxn}}^{\circ} = 1,430,600 - 803.25T \text{ (J)} \quad (11)$$

Similarly, other reactions that form transition metal borides from oxide precursors, Reactions 4 and 5, also become favorable at elevated temperature and are highly endothermic. Comparison of the values of $\Delta G_{\text{rxn}}^{\circ}$ for Reactions 1, 4, and 5 normalized to formation of one mole of ZrB₂

shows that each becomes favorable between 1300°C and 1500°C, Figure 1.¹⁰³ Hence, selecting different precursors does not necessarily affect the temperature required for formation, but can impact the resulting particle morphology or reaction efficiency.

An interesting variation of carbothermal synthesis of borides has been utilized to densify TM diborides. Baik and Becher were the first to observe that densification of TiB_2 was enhanced by decreasing the oxygen content of the starting powder.¹⁰⁴ Subsequently, Chamberlain observed that ZrB_2 containing WC impurities could be densified by pressureless sintering and attributed the enhanced densification to the removal of surface oxide impurities by reaction with WC.¹⁰⁵ In addition, carbon,¹⁰⁶ carbides,^{107-108,109} nitrides,^{110,111} and combinations of these additives^{112,113} have all been identified as sintering aids for TM diborides based on their ability to react with and remove oxide impurities from the surface of diboride powder particles. The mechanism for oxygen removal from ZrB_2 was studied by Zhu et al.¹⁰⁶ and is summarized by the schematic in Figure 2. Hence, carbothermal reduction reactions can not only be used to form boride or carbide phases, but can also be harnessed to enhance densification of pre-reacted TM diborides by removing surface oxide impurities that promote preferential coarsening rather than densification.

Both borothermal and boro/carbothermal reduction reactions can also be used to produce boride powders. The former involves a pure source of boron, which is usually more expensive than carbon and requires a higher reaction temperature. The main advantage of borothermal reduction is the purity of the final powders and the potential for achieving a fine particle size.¹¹⁴ For example, borothermal reduction of HfO_2 at 1100°C, followed by washing with hot water and the removal of residual B_2O_3 at 1550°C yielded powders with ~0.56 wt% O_2 and a particle size in the range of 0.5 to 1 μm .¹¹⁴ Addition of excess B, whilst keeping the synthesis conditions the

same, resulted in lowering of the O content to just 0.51 wt%. Other work on the densification of $\text{ZrB}_2\text{-SiC}$ ceramics with additional B also showed that the latter can reduce oxygen impurities and enhance the densification process.¹¹⁵ High-purity ZrB_2 powders with submicron particle size have also been synthesized by borothermal reduction of nanometric ZrO_2 powders in vacuum.¹¹⁶ The ZrO_2 completely converted to ZrB_2 at 1000°C , but removal of residual boron species required temperatures above 1500°C . In addition, powders obtained at $1000\text{-}1200^\circ\text{C}$ were ~ 150 nm and showed a faceted morphology, whereas those prepared above 1500°C were coarser, typically $\sim 0.66\text{ }\mu\text{m}$, with a nearly spherical morphology. The oxygen content of the ZrB_2 powders synthesized at 1650°C was as low as 0.43 wt%.

Carbo/borothermal reduction uses the combination of B_4C and C as reducing agents. The temperature at which such reductions are initiated can be quite low, e.g. 1200°C for ZrB_2 ,¹¹⁷ though to yield high-purity powders a higher heat treatment temperature was needed. The carbo/borothermal reduction reaction has also been exploited to promote densification of ZrB_2 due to the ability of excess B_4C to react with oxides and thereby reduce the amount of oxide impurities in the non-oxide ceramics.¹⁰⁷

IV. Reactive Processes

Direct synthesis and displacement reactions are also widely employed to produce boride ceramics. Compared to oxides, starting from pure metals or metal compounds provides the ability to control impurity levels in the resulting ceramics. For example, a series of ZrB_2 ceramics with Hf contents ranging from ~ 0.01 at% to 0.33 at% were produced by reactive hot pressing.¹⁰¹ Reactive processes can be used to design boride ceramics, particularly on the laboratory scale. Furthermore, reactive synthesis is routinely combined with densification into a single, *in-situ* process to produce dense ceramics¹¹⁸⁻¹²¹ or fiber reinforced composites.¹²²

Ceramics could be densified at a relative lower temperature by reactive sintering, as a result of the newly formed fine powder with a higher sinterability and a lower oxygen content, which was generated from these *in-situ* reactions.

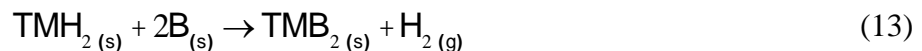
A. Direct Reaction of Elements, Hydrides, or Chlorides

The formation of transition metal boride compounds from elemental precursors (Reaction 2) is highly favorable. For example, the reaction of zirconium and boron to produce ZrB_2 is thermodynamically favorable at room temperature ($\Delta G_{\text{rxn}}^{\circ} = -319 \text{ kJ}$ at 298 K) and the process is highly exothermic ($\Delta H_{\text{rxn}}^{\circ} = -323 \text{ kJ}$ at 298 K). Because they are highly exothermic, these reactions also have extremely high adiabatic temperatures, T_{ad} . For the reaction of Zr and B to form ZrB_2 , T_{ad} is $\sim 3100 \text{ K}$. Previous empirical analysis has concluded that self-propagating high-temperature synthesis (SHS) can initiate for reactions when $T_{\text{ad}} > 1800 \text{ K}$, indicating that an SHS reaction is likely for the reaction of TMs and B by Reaction 2. Although the latter is highly favorable at room temperature, kinetic limitations require elevated temperatures for the reaction to proceed. No ZrB_2 was detected after attrition milling of Zr and B powders at a speed of 600 rpm up to 4h when the milling container remained at room temperature.¹²³ In this case, reaction required further heat treatment of milled powders at temperatures above 600°C , but the reaction occurred over a broad range of temperatures. In contrast to the attrition milling studies, mechanical alloying using planetary milling at 250 rpm for 20 hr in argon resulted in ZrB_2 formation during milling.¹²⁴ However, the temperature inside the chamber was not monitored during milling. Together, these studies revealed that reducing the size of the elemental precursors reduced the onset temperature for reaction, as expected.

The reaction between TMs and B proceeds by diffusion of B atoms through the TMB_2 reaction layer to react with the TM. Figure 3.¹²³ The preferred diffusion path for B atoms is

octahedral site (Oct)-basal bond center (Bc)-Oct, which was identified using nudged elastic band simulations.¹²⁵ The latter also revealed that the Oc-Bc-Oct mechanism had a lower energy by a factor of ~20 compared to the next most favorable process. Building on these findings, the morphology of TMB₂ produced by Reaction 2 is strongly influenced by the shape and size of starting TM powder particles. As shown in Figure 4a and b, ZrB₂ with spherical morphology was synthesized directly from elements using precursors with sizes in the range of 200 nm to 1 μm.^{123,124,126} Anisotropic grain growth can be promoted through additions to the starting powder mixture. For example, ZrB₂ grains showing preferred growth along the a- and/or b-axes was achieved by adding Si and a TM such as Mo, Nb, Ti, or W into the initial Zr and B powder mixture, Figure 4c.¹²⁷ Not only can reactive methods help control the shape of the particles, but they also provide control over particle size.

Because they are brittle, the size of B particles can be reduced by conventional milling processes.¹²⁸ In contrast, milling of ductile TM particles typically results in the formation of thin platelets or flakes due to the strong shearing forces during attrition or planetary milling.^{123,129} Extended milling times can result in the incorporation of impurities from the milling media, which can affect the reactions, densification behavior, and properties of the resulting ceramics. To reduce milling times and, therefore, limit impurity incorporation, brittle compounds such as TM chlorides, Reaction 9, or hydrides, Reaction 13, can be used as precursors for synthesis reactions.¹³⁰⁻¹³²



Thermodynamically, ZrH₂ can be spontaneously dehydrogenated to metallic Zr during heating. In the standard state (assuming unit activity for condensed phases and a partial pressure of 101 kPa for H₂), the decomposition of ZrH₂ is favorable above ~975°C. Because the partial pressure

of hydrogen is typically drastically lower than 101 kPa, the reaction can become favorable at much lower temperatures. For example, the Gibbs change for dehydrogenation becomes negative at $\sim 510^{\circ}\text{C}$ under 10 Pa of H_2 gas. In the presence of B, Reaction 13, the formation of ZrB_2 is favorable across a broad range of temperatures regardless of the partial pressure of H_2 , indicating that ZrB_2 formation should occur simultaneously with ZrH_2 decomposition as compared to a sequential process in which ZrH_2 decomposes at one temperature followed by ZrB_2 formation at a second higher temperature. Ran¹³¹ and Guo¹³⁰ separately observed that ZrH_2 dissociation occurred between 600°C and 1300°C , depending on the particle size of ZrH_2 and the decomposition conditions. Kinetically, dehydrogenation of ZrH_2 follows occurs in steps (e.g., $\text{ZrH}_2 \rightarrow \text{ZrH}_m$ ($m < 2$) $\rightarrow \text{Zr}$), which results in separate endothermic peaks at 700°C and 1300°C in differential scanning calorimetry.¹³⁰ Guo's conclusion was that ZrB_2 formation occurred in steps whereas Ran hypothesized that dehydrogenation and reaction occurred in a single step at a fixed temperature. Heating rate may also have an effect on reaction. Heating ZrH_2 -B mixtures at $100^{\circ}\text{C}/\text{min}$ to 900°C resulted in the formation of ZrB_2 with a primary crystallite size of ~ 100 nm, Figure 4d and 4e.¹³¹ Together, previous studies show that TMb_2 with high purity can be formed by synthesis from metals or hydrides and that these processes provide control over particle size and shape.

Unlike TMH_2 compounds, TMCl_4 sublimates prior to decomposition. For ZrCl_4 , sublimation is favorable above $\sim 340^{\circ}\text{C}$ for standard state conditions. In typical synthesis processes, powder mixtures will be heated in vacuum or inert atmosphere, which will shift sublimation to even lower temperatures. Although thermodynamic calculation show that reaction between solid ZrCl_4 and B is favorable below 300°C , TMb_2 powders have not been reported to be produced by direct reaction of solid chlorides with B. In addition to the vapor

phase routes, TMCl_4 compounds can readily hydrolyze to oxides (TMO_2) or oxychlorides (TMOCl_2), which can then react with B in the solid state. For example, Guo produced ZrB_2 powders consisting of plate-like particles and whiskers by reaction of hydrolyzed ZrCl_4 at 1200°C .¹³²

Chemical exchange (metathesis) reactions have also been used to produce borides from transition metal halides. Operating in a similar manner to SHS reactions discussed above, the basic form of the reaction is: $\text{AB} + \text{CD} \rightarrow \text{AC} + \text{BD}$. Borides have been produced, for example, by reaction a transition metal chloride with MgB_2 .¹³³⁻¹³⁵ In general, such metathesis reactions can yield rapid, highly exothermic reactions with temperatures $>1000^\circ\text{C}$ on very short time scales of <1 s. The products are often crystalline and single phase with crystallite sizes varying from tens of angstroms to a few microns, depending on the refractory nature of the material and the reaction conditions (i.e., scale and the use of inert additives). For the reaction between TMCl_4 and MgB_2 , it has been reported to occur above 650°C in an evacuated silica tube. However, apart from TMB_2 and MgCl_2 , boron was also detected in addition to the TMB_2 and MgCl_2 so these routes can struggle to yield phase pure products.¹³³

To summarize this section, direct synthesis reactions have been widely used to produce TM boride ceramics. Precursors can include metals, TM hydrides, or TM compounds. These routes are highly advantageous on the laboratory scale due to the ability to control the purity of the resulting ceramic powders in addition to providing compositional flexibility and reduced particle sizes. These reactions tend to be highly exothermic, but SHS type-reactions can be inhibited by adding inert diluents or using slow heating rates. Further development of appropriate precursors and control of process parameters would be necessary to extend these methods to practical powder production routes on larger scales.

B. Displacement Reactions

Displacement reactions are another common method used for *in-situ* synthesis of ceramics and composites.¹²¹ These reactions offer the same advantages as direct synthesis reactions (e.g., low temperatures, high purity, control of particle morphology), but often using less costly or more stable precursors. The section below separately considers reactions involving TM metals and TM compounds such as carbides or nitrides.

Pure TMs can react with B-containing inorganic compounds. Some examples of reactions, thermodynamic favorability, and reaction conditions for the production of ZrB₂-containing materials are summarized as Reactions 14-22 in Table III.¹³⁶¹⁴⁴ Reaction 14 has been widely investigated to produce ZrB₂-SiC ceramics.^{118,145-147} When batched according to the reaction stoichiometry, the reaction produces 74.9 vol% ZrB₂ and 25.1 vol% SiC, although the ratio can be adjusted by adding either ZrB₂ or SiC into the precursors.¹¹⁸ Furthermore, the ratio of the precursors can be altered as described by Reaction 15 to introduce ZrC as a reaction product.¹⁴⁸ Likewise, HfB₂ ceramics containing 22 vol% SiC and 5 vol% ZrC can be synthesized below 1200°C from a mixture of Hf, Si, and B₄C.¹⁴⁹

Overall, Reaction 14 leads to the formation of ZrB₂ and SiC. However, analysis of the reaction path revealed that ZrC formed prior to ZrB₂ as an intermediate product at temperatures as low as 800°C.¹⁴⁸ The preferential formation of ZrC at moderate temperatures was attributed to the lower activation energy for diffusion of C in Zr (~75 kJ/mole) compared to diffusion of B in Zr (~145 kJ/mole).¹⁴⁴ Qu et al. suggested that the intermediate carbide was carbon-deficient (e.g., ZrC_x with $x < 1$) due to diffusion limitations during reaction.¹⁴⁴ Similarly, ZrC_x was also formed by incorporating excess Zr into ZrC.¹⁴² Above 1100°C, XRD analysis suggested that the amount of ZrC decreased gradually with increasing temperature, indicating that ZrC reacted with

residual B₄C and Si to form ZrB₂ and SiC, Reaction 22. By 1500°C, ZrB₂ formation was complete, but ZrC could be retained in the final powder mixture depending upon the Zr to B₄C ratio, Reaction 15.



The kinetics of Reaction 14 and 15 can be manipulated by controlling the processing conditions.^{144,150,151} During SHS reactions ignited by rapid heating of Zr-Si-B₄C mixtures, Reaction 14 appeared to proceed in one step.¹⁵¹ Particle size also had an effect on reaction as demonstrated by Wu et.al who observed an increase in gas pressure at ~900°C during heating of fine Zr and B₄C, while no pressure change on vacuum was monitored for coarse powders.¹⁵⁰ Interestingly, densification behavior also benefited from the lower reaction temperature as dense ZrB₂-SiC-ZrC ceramics were produced at 1600°C for fine powders compared to temperatures at least 200°C higher for reaction of coarse powders.¹⁵⁰

In a variation of SHS, Reaction 15 has been ignited using an infrared lamp as a heat source.¹⁵¹ Combustion could be ignited when the Zr-B₄C-Si mixture was heated in air, but not in argon. Interestingly, the powders produced by combustion in air had a lower oxygen content (0.4 wt%) than typical commercial powders, which contain 1 wt% oxygen or more. Analysis showed that the infrared lamp only heated the powder surface to ~100°C in air or in argon, so ignition of the SHS reaction was attributed to the exothermic oxidation of Zr when powders were heated in air.¹⁵¹ Similarly, ZrB₂-ZrC powders were synthesized by SHS that was ignited by exposing finely ground Zr-B-C powder mixture to air at room temperature.^{152,153} After SHS, the powders are typically agglomerated, although deagglomeration can be achieved by ball milling. In additions, powders produced by SHS can exhibit better sinterability compared to conventional powders due to finer particle size or increased defect concentrations.¹⁴⁴

In another variation, replacing the Si in Reaction 14 with Si₃N₄ results in production of ZrB₂-SiC ceramics that also contained BN, Reaction 18.¹⁵⁴ These ceramics had an excellent combination of high strength (>600 MPa) and machinability. Additional variations in precursor chemistry and the resulting phases are summarized in Reactions 23-25. Similarly, TMC and TMN can also be used as precursors for the preparation of TMB₂-based ceramics. Thermodynamic analysis indicates that neither TM carbides nor TM nitrides are stable in contact with boron compounds at elevated temperatures. Reactions 22-24 are representative displacement reactions for synthesis of ZrB₂-based ceramics from carbide and nitride precursors.



Rapid heating of the precursors for Reactions 23-25 can result in ignition of SHS reactions between 1300°C and 1400°C.^{155,156} In general, an SHS reaction produces local extreme temperatures (e.g., approaching T_{melt} for one or more of the product phases) for a short duration (e.g., a few seconds). As a result, fine powders produced by SHS can be partially sintered, which produces hard agglomerates and decreasing sinterability. Reactions 23-25 are classified as “mild” SHS reactions because T_{ad} is below 1800°C.¹⁵⁰ As a consequence, the resulting ZrB₂-B₄C powder mixtures can be densified below 1800°C.¹⁵⁰ Not only can displacement reactions be used to produce sinterable powders, but the reactions can also provide increased control over the morphology of the resulting powders, Figure 5.¹⁵⁶ Although the mechanisms have not been confirmed, the authors speculated that nucleation of the product phases at defects in the coarse precursor particles resulted in a substantial reduction in the size of the resulting powders compared to the size of the precursors.¹⁵⁶ Similar reductions in grain size were observed for

synthesis of $\text{TiB}_2\text{-B}_4\text{C}$ ceramics. For example, Reaction 23 was used to synthesize particles with an average size of ~ 50 nm at 1200°C and to produce ceramics in the Ti-B-C system.^{157,158}

Both TiB_2 and ZrB_2 have also been formed at room temperature via the mechanical milling of a mixture of Mg, B_2O_3 and the corresponding TM oxide under vacuum and argon respectively for up to 15 h in a laboratory scale ball mill.^{159,160} X-ray diffraction analysis showed increasing conversion with milling time, eventually leading to phase-pure borides as detected by XRD. For ZrB_2 , differential thermal analysis revealed multiple overlapping reactions, all of which seemed to be related to TM boride formation. After milling, separation of the boride from the MgO co-product was achieved by a mild acid leaching, leaving essentially pure boride powders with crystallite sizes of <100 nm. Similar results were obtained for TiB_2 by Ricceri et al. using high-energy ball milling for ~ 1 hr.¹⁶¹ They hypothesized that two nearly simultaneous thermite reactions occurred, one between TiO_2 and Mg and the other between B_2O_3 and Mg; the first provided sufficient heat to ignite the second. These reactions were immediately followed by reaction between elemental Ti and B to provide TiB_2 . XRD revealed a gradual decrease in crystallite size of the reactant TiO_2 , with formation of intermediate reaction products followed by a near-instantaneous reaction that produced mainly MgO and TiB_2 as final products. Intermediate reaction products, such as less stable borides, were retained for shorter milling times, but TiB_2 and MgO were the only products for milling times of 2 h. After removal of MgO by leaching in dilute HCl, pure TiB_2 was obtained with a typical molar yield of 81%. The powders were impact-welded aggregates composed of 50–100 nm particles. It is possible that a similar approach could also lead to the self-propagation formation of ZrB_2 .

Overall, displacement reactions are a highly attractive synthesis route for multiphase ceramics. Displacement reactions afford the ability to produce TM boride-based ceramics

containing additional hard phases such as SiC, ZrC, or B₄C that limit grain growth and improve physical and/or mechanical properties. In addition, precursors can also be designed to produce phases such as BN that improve fracture toughness or machinability. Hence, displacement reaction-based processes can be used to tailor the composition, microstructure, and properties of TM boride ceramics.

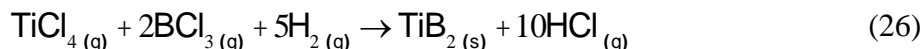
V. Chemical Synthesis

A broad range of chemical synthesis methods have been used to produce boride powders on the laboratory scale when highly pure and/or extremely fine particles are needed. For comparison to the methods discussed in previous sections, reduction-based processes, which are predominantly used for commercial synthesis of boride powders due to simplicity and low cost, yield coarse particles with low sinterability.¹⁶² Considerable grinding is required for particle size reduction, which can result in the incorporation of impurities. Likewise, the size of the end product for reaction-based processes depends on the size of the precursors; thus they are usually milled before reaction. Hence, research that aims to produce highly pure and/or extremely fine powders typically utilizes chemical synthesis routes. In addition to synthesis solely involving chemical processes, this section discusses hybrid processes that combine chemical (typically solution) routes with other processes such as direct reactions or carbothermal reduction.

Figure 6¹⁶³ summarizes the broad range of reactions for synthesis of HfB₂, several of which are possible below 1500°C. Various reactions other than borothermal and carbothermal reduction reactions, using elemental Hf or its carbide or nitride, lead to successful synthesis. These reactions allow for use of combinations of polymeric precursors and reactive powders to synthesize group IV metal borides. All of the reactions need to be considered during design and

development of practical precursor processing as intermediate reactions and their products may play a key role in obtaining the desired phases and microstructures.

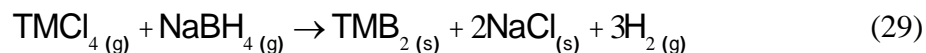
Most chemical routes involve reactions between TM-containing and B-containing precursors. For example, a principle synthesis route for TiB₂ involves reduction of titanium tetrachloride and a boron halide at ~1500°C, Reaction 26, although the solid diboride product requires grinding.¹⁶²



Boride powders can also be formed by decomposition of borohydrides. Ti(BH₄)₃ was first synthesized as long ago as 1949 by passing TiCl₄ vapor over lithium borohydride, Reaction 27,¹⁶⁴ whilst nearly a decade later Ti(BH₄)₃ was prepared by bubbling diborane, B₂H₆, through a titanium butoxide solution in tetrahydrofuran.¹⁶⁵ Interestingly, Ti(BH₄)₃ decomposes at ~140°C when dissolved in xylene, Reaction 28.¹⁶⁶ Whilst the resulting powder was agglomerated, it had a high chemical purity and a particle size in the range of 100 to 200 nm.



Nano-crystalline ZrB₂ and HfB₂ have been synthesized by Reaction 29 at temperatures of 500-700°C and 600°C, respectively, using a hydrothermal reaction in an autoclave.^{167,168} These studies make no mention of the purity of the final powder, which is a concern because sodium-bearing compounds are usually not ideal for producing engineering ceramics since the presence of alkali metals is detrimental to the subsequent properties. Nevertheless, these are amongst the lowest synthesis temperatures reported for these borides via an elevated temperature reaction. The particle sizes were reported to be as fine as 10-25 nm in both cases.¹⁶⁷⁻¹⁶⁸



Boride powders have also been synthesized via sol-gel processing followed by carbothermal reduction. Molecular level mixing in the liquid form allows transformation to the final product at lower temperatures than by many other routes with improved homogeneity of the final product. Yan et al. prepared high-purity ZrB₂ with particle sizes from 100 – 200 nm, Figure 7, using inorganic–organic hybrid precursors of zirconium oxychloride (ZrOCl₂•8H₂O), boric acid and phenolic resin as sources of zirconia, boron oxide and carbon, respectively.¹⁶⁹ The reactions were substantially completed at the relatively low temperature of ~1500°C. The synthesized powders had a smaller average crystallite size (<200 nm), larger specific surface area (~32 m²g⁻¹) and lower oxygen content (<1.0 wt%) than for many commercially available ZrB₂ powders. Ultra-fine TiB₂ powders have also been prepared by sol-gel processing with tetrabutyl titanate, boric acid and phenolic resin as the solution precursors.¹⁷⁰ The carbothermal reduction reactions were substantially completed below 1400°C. At temperatures below 1100°C, titanium carbide was the predominant phase and the resulting products consequently had a fine average crystallite size of <200 nm. A sol-gel mixture of HfCl₄, H₃BO₃ and phenolic resin was used to obtain intimately mixed, yet unreacted, HfO₂, B₂O₃ and C, which was calcined to produce HfB₂.¹⁷¹ Usually this approach results in minor impurities such as HfO₂, HfC and B₄C in the final product; in this study the ratios of the different precursors were optimized to obtain HfB₂ powder with negligible impurities. Calcination at temperatures as low as 1300°C produced HfB₂, but required 25 h to form pure phase HfB₂. The long dwell time gave rise to a significant fraction of rod shaped particles, with screw dislocation driven growth occurring along the c-axis.¹⁷² The use of a higher calcination temperature avoided this problem.

Carbon sources with different structures were studied to produce HfB₂ particles with different size and morphology using HfCl₄ and H₃BO₃ as precursors. The carbon sources included liquid phenolic resin, phenolic resin powder, pitch, sucrose, graphite, carbon black, and carbon nanotubes.¹⁷³ In general, the structure and level of agglomeration of the carbon source influenced the particle size of HfB₂ powder, Figure 8. For example, carbon black and carbon nanotube precursors produced HfB₂ particles whose size directly depended on the level of agglomeration of carbon sources whilst, on pyrolysis, the liquid phenolic resin, sucrose, graphite and powder phenolic resin all resulted in sheet-like carbon that engulfed the ceramic particles. Finer and more dispersed sheets produced finer and less agglomerated HfB₂ particles. The finest HfB₂ powder was obtained when using phenolic resin powder as the carbon source, which resulted in a final particle size between 30 and 150 nm with a surface area of 21.8 m²/g.

Duplex submicron ZrB₂-SiC powders have been synthesized *in-situ* via a combined sol-gel and microwave boro/carbothermal reduction route, Figure 9.¹⁷⁴ Additives such as SiC, MoSi₂, LaB₆, WC, TaC, TaSi₂ and TaB₂ are commonly used to improve the performance of TM borides in high temperature applications,¹⁷⁵⁻¹⁷⁸ although they are typically added as a second phase during powder processing.¹⁷⁹⁻¹⁸² The most widely studied additive is SiC, which reduces the oxidation rate of TM borides by forming a borosilicate layer on the surface during oxidation at temperatures below 1600°C.¹⁸³⁻¹⁸⁵ Using chemical methods, the optimum molar ratios were determined to be $n(B)/n(Zr) = 2.5$ and $n(C)/n(Zr+Si) = 8$. Chemical synthesis reduced the calcination temperature to only 1300°C, which was ~200°C lower than conventional methods. Examination of microstructures and phase morphologies revealed a mixture of particles with three different chemistries, morphologies, and sizes. A sizeable fraction of 1-2 µm columnar ZrB₂ grains were in a matrix consisting of ~500 nm granular particles mixed in with numerous

<100 nm particles. Both of the latter contained Zr, B, Si and C, which was interpreted to be a ZrB₂-SiC composite powder in which SiC grains were distributed evenly amongst ZrB₂ grains. ZrB₂-SiC duplex powders with different morphologies have also been synthesized from amorphous hydrous ZrO₂-SiO₂ produced by precipitation and sol-gel processing.¹⁸⁶ Calcining at 1500°C resulted in formation of the desired phases. The powder derived from the precipitation route consisted of rod-like ZrB₂ with smaller, irregular SiC particles adhering to them while the sol-gel route yielded equiaxed particles in which both ZrB₂ and SiC were evenly distributed.

Chemical synthesis routes have also been used to produce TM borides doped with group IV and V metals. Dopants have been shown to modify the morphology of the crystalline phase in the oxide scale and reduce the oxygen permeation rate.¹⁸⁷⁻¹⁸⁹ Dopants such as Ti, Nb, and Ta, form continuous solid solutions with ZrB₂,^{190, 191} with solid solution formation limited by diffusion of TM atoms. Hence, activation energies for metal diffusion correlate to the ease of forming a solid solution. Activation energies are 112 kJ/mole for ZrB₂-TiB₂, 175 kJ/mole for TiB₂-NbB₂ and 400 kJ/mole NbB₂-CrB₂, which have atomic radii differences of 1% for Ti and Nb; 9% for Zr and Ti; and 13% for Nb and Cr.¹⁹² Note that the latter does not form a continuous solid solution. Uniform distribution of the dopants is desired and chemical synthesis routes are more successful for introducing dopants than solid state mixing techniques. For example, when milling was used to mix commercially available ZrB₂ and TaB₂ powders, samples required hot pressing at 1900-2000°C¹⁷⁸. In contrast, Xie used tantalum ethoxide and zirconium n-propoxide dissolved into solution in 2,4-pentanedioneas to produce precursors that converted to solid solution (Zr,Ta)B₂ powders at only 1600°C due to the homogeneous distribution of the metal cations.¹⁷⁵ Co-precipitation is another approach that promotes distribution of dopants in boride powders, though this requires precise control of the pH values to precipitate the dopant and

matrix simultaneously. Jiang¹⁹³ used this route to synthesize $\text{ZrO}_2\text{-WO}_3$ precursors that were subsequently reacted with amorphous boron at 1550°C to produce W-doped ZrB_2 powders with a mean particle size of ~ 400 nm. Besides borides and W, chemical synthesis has also been used to dope other Group IV and V refractory metal compounds, such as TaSi_2 , TaC and WC , into HfB_2 and ZrB_2 ¹⁹⁴⁻¹⁹⁸. These carbide and silicide dopants can be partially reduced by boron and become mutually soluble with the host matrices, hence modifying the crystalline phase in the oxide scale as for the additions of one boride to another.

Chemical synthesis routes are attractive due to the ability to control the purity and particle size of the resulting TM boride powders. In addition, these methods can be used to uniformly distribute second phases or dopants at temperatures significantly lower than conventional powder process. Although these methods are only used at the laboratory scale presently, they have the potential for widespread use in applications that demand uniform, highly sinterable powders with controlled compositions.

VI. Summary and Outlook

Synthesis methods for boride ceramics have been reviewed. While these methods can be generally used for many different boride compounds, this review emphasized methods applicable to TM diboride ceramics. Initial reports of the discovery of TM diboride compounds describe the formation of impure multiphase materials. Purification of boron enabled the isolation of phase-pure TM diborides, although present-day commercial production typically utilizes carbothermal reduction of TM oxides and boric acid based on cost considerations. Laboratory scale syntheses by reactive methods or chemical routes allows for precise control of particle size and purity for fundamental studies, although these methods have not proved commercially viable to date. The choice of methods for synthesis can be made based on a balance of cost with the

properties of the resulting powders with the most important properties being starting particle size, purity, and oxygen content.

In the future, continued research into synthesis methods will be driven by the need for materials that exhibit improved performance in extreme environments, higher purity for improved properties, or smaller particle size for enhanced densification and control of final microstructure. As such, interest in all of the synthesis methods discussed in this review should continue to increase. At the same time, continual increases in operating temperatures in applications that strive for increased energy efficiency or revolutionary changes in performance will continue provide motivation to synthesize boride compounds with improved properties. Hence, future research will likely increasingly focus on existing and emerging methods that produce ceramic powders with sub-micron particle sizes, metallic impurity contents in the part-per-million range, and oxygen impurity contents below one weight percent.

Acknowledgments

This manuscript was conceived and drafted as part of an extended visit by WGF to the University of Birmingham during the spring of 2015. The authors wish to thank the U.K. Engineering and Physical Science Research Council (EPSRC) for financial support through the Materials Systems for Extreme Environments (XMAT) program.

Reference

1. Unless otherwise noted melting temperatures are from Alloy Phase Diagrams: ASM Handbook Volume 3, ASM International, Materials Park, OH, 1992.
2. All data on space groups and density were taken from the PDF-2 Database, International Centre for Diffraction Data, Newtown Square, PA.
3. S. Madtha, C. Lee, and K.S. Ravi Chandran: Physical and Mechanical Properties of Nanostructured Titanium Boride (TiB) Ceramic. *Journal of the American Ceramic Society*, 91, 1319 (2008).
4. L. Sun, Y. Gao, B. Xiao, Y. Li, and G. Wang: Anisotropic Elastic and Thermal Properties of Titanium Borides by First Principles Calculations. *Journal of Alloys and Compounds*, 579, 457 (2013).

5. K.B. Panda and K.S. Ravi Chandran: First Principles Determination of Elastic Constants and Chemical Bonding of Titanium Boride (TiB) on the Basis of Density Functional Theory. *Acta Materialia*, 54, 1641 (2006).
6. A.L Chamberlain, W.G. Fahrenholtz, G.E. Hilmas, and D.T. Ellerby: High Strength ZrB₂-Based Ceramics. *Journal of the American Ceramic Society*, 87, 1170 (2004).
7. N.L. Okamoto, M. Kusakari, K. Tanaka, H. Inui, and S. Otani: Anisotropic Elastic Constants and Thermal Expansivities in Monocrystal CrB₂, TiB₂, and ZrB₂. *Acta Materialia*, 58, 76 (2010).
8. P. Rogl and P.E. Potter: A Critical Review and Thermodynamic Calculation of the Binary System: Hafnium-Boron. *CALPHAD*, 12, 207 (1988).
9. Figure III.C.3.1, page 202 in E. Rudy, "Ternary Phase Equilibria in Transition Metal-Boron-Carbon-Silicon Systems: Part V. Compendium of Phase Diagram Data," Technical Report Number AFML-TR-65-2, Air Force Materials Laboratory, Wright-Patterson Air Force Base, May 1969
10. K. Sairam, J.K. Sonber, T.S.R.Ch. Murthy, C. Subramanian, R.K. Fortedar, and R.C. Hubi: Reaction Spark Plasma Sintering of Niobium Diboride. *International Journal of Refractory Metals and Hard Materials*, 43, 259 (2014).
11. M. Zhang, H. Wang, H. Wang, T. Cui, and Y. Ma: Structural Modifications and Mechanical Properties of Molybdenum Borides from First Principles. *Journal of Physical Chemistry C*, 114, 6722 (2010).
12. H.-H. Chen, Y. Bi, Y. Cheng, G. Ji, and L. Cai: Elastic Stability and Electronic Structure of Tantalum Boride Investigated via First-Principles Density Functional Calculations. *Journal of Physics and Chemistry of Solids*, 73, 1197 (2012).
13. X. Zhang, G.E. Hilmas, and W.G. Fahrenholtz: Synthesis, Densification, and Mechanical Properties of TaB₂. *Materials Letters*, 62, 4251 (2008).
14. W. J. Zhao and Y.X. Wang: Structural, Mechanical, and Electronic Properties of TaB₂, TaB, IrB₂, and IrB: First Principles Calculations. *Journal of Solid State Chemistry*, 182, 2880 (2009).
15. H. Duschaneck and P. Rogl: Critical Assessment and Thermodynamic Calculation of the Binary System Boron-Tungsten. *Journal of Phase Equilibria*, 16, 150 (1995).
16. Y. Chen, D. He, J. Qin, Z. Kou, S. Wang, and J. Wang: Ultrahigh-Pressure Densification of Nanocrystalline WB Ceramics. *Journal of Materials Research*, 25, 637 (2010).
17. E. Zhao, J. Meng, Y. Ma, and Z. Wu: Phase Stability and Mechanical Properties of Tungsten Borides from First Principles Calculations. *Physical Chemistry and Chemical Physics*, 12 13158 (2010).
18. H. Guo, Z. Li, J. Zhang, H. Niu, F. Gao, R.E. Ewing, and J. Lian: Origin of the Rigidity in Tetragonal MB (M = Cr, Mo, and W) and Softening of Defective WB: First Principles Investigations. *Computational Materials Science*, 53, 460 (2012).
19. J. Qin, D. He, J. Wang, L. Fang, Y. Li, J. Hu, Z. Kou, and Y. Bi: Is Rhenium Diboride a Superhard Material?. *Advanced Materials*, 20 4780 (2008).
20. M. Hebbache, L. Suparevic, and D. Zivkovic: A New Superhard Material: Osmium Diboride OsB₂. *Solid State Communications*, 139 227 (2006).
21. H.-Y. Chung, Y.-M. Yang, S.H. Tolbert, and R.B. Kaner: Anisotropic Mechanical Properties of Ultra-Incompressible Hard Osmium Diboride. *Journal of Materials Research*, 23 1797 (2008).

22. A.L. Ivanovskii: Mechanical and Electronic Properties of Diborides of Transition 3d-5d Metals from First Principles: Toward Search of Novel Ultra-Incompressible and Superhard Materials. *Progress in Materials Science*, 57, 184 (2012).
23. Y. Zhou, J. Wang, Z. Li, X. Sun, and J. Wang: First-Principles Investigation on Anisotropic Chemical Bonding and Elastic Properties of Transition Metal Diborides TMB_2 (TM = Zr, Hf, Nb, Ta, and Y). pp. 60-82 in Ultra-High Temperature Ceramics: Materials For Extreme Environment Applications, ed. by W.G. Fahrenholtz, E.J. Wuchina, W.E. Lee, and Y. Zhou, Wiley, New York, 2014.
24. A.L. Ivanovskii, I.R. Shein, and N.I. Medvedeva: Non-Stoichiometric s-, p-, and d-Metal Diborides: Synthesis, Properties, and Simulation. *Russian Chemical Reviews*, 77 467 (2008).
25. P. Vajeeston, P. Ravindran, C. Ravi, and R. Asokamani: Electronic Structure, Bonding, and Ground-State Properties of AlB_2 -Type Transition-Metal Diborides. *Physical Review B*, 63, 045115-1 (2001)
26. G. Harrington, G.E. Hilmas, and W.G. Fahrenholtz: Effect of Carbon on the Thermal and Electrical Transport Properties of Zirconium Diboride. *Journal of the European Ceramic Society*, 35, 887 (2015).
27. S. Guo, T. Nishimura, and Y. Kagawa: Preparation of Zirconium Diboride Ceramics by Reactive Spark Plasma Sintering of Zirconium Hydride-Boron Powders. *Scripta Materialia*, 65, 1018 (2001).
28. J.M. Lonergan, W.G. Fahrenholtz, and G.E. Hilmas: Zirconium Diboride with High Thermal Conductivity. *Journal of the American Ceramic Society*, 97, 1689 (2014).
29. L. Zhang, D.A. Pejaković, J. Marschall, and M. Gasch: Thermal and Electrical Transport Properties of Spark Plasma-Sintered HfB_2 and ZrB_2 Ceramics. *Journal of the American Ceramic Society*, 94, 2562 (2011).
30. R.A. Andrievski: Superhard Materials Based on Nanostructured High-Melting Point Compounds: Achievements and Perspectives. *International Journal of Refractory Metals and Hard Materials*, 19, 447 (2001).
31. B. Basu, G.B. Raju, and A.K. Suri: Processing and Properties of Monolithic TiB_2 -Based Materials. *International Materials Reviews*, 51, 352 (2006).
32. X. Zhang, X. Luo, J. Han, J. Li, and W. Han: Electronic Structure, Elasticity, and Hardness of Diborides of Zirconium and Hafnium: First Principles Calculations. *Computational Materials Science*, 4, 411 (2008).
33. J.W. Lawson, C.W. Bauschlicher, Jr., and M.S. Daw: Ab-Initio Computations of Electronic, Mechanical, and Thermal Properties of ZrB_2 and HfB_2 . *Journal of the American Ceramic Society*, 94, 3494 (2011).
34. S.Q. Guo: Densification of ZrB_2 -Based Composites and Their Mechanical and Physical Properties: A Review. *Journal of the European Ceramic Society*, 29 995 (2009).
35. E. Wuchina, M. Opeka, S. Causey, K. Buesking, J. Spain, A. Cull, J. Routbort, and F. Guitierrez-Mora: Designing of Ultrahigh-Temperature Applications: The Mechanical and Thermal Properties of HfB_2 , HfC_x , HfN_x , and $\alpha Hf(N)$. *Journal of Materials Science*, 39, 5939 (2004).
36. P. Kolodziej, J. Salute, and D.L. Keese: First Flight Demonstration of a Sharp Ultra-High Temperature Ceramic Noisetip. *NASA Technical Report TM-112215*, December 1997.
37. E.L. Courtright, H.C. Graham, A.P. Katz, and R.J. Kerans: Ultra-High Temperature Assessment Study—Ceramic Matrix Composites. *Final Report WL-TR-91-4061*, Wright

Laboratory Materials Directorate, Wright Patterson Air Force Base, Dayton, OH, September 1992.

38. D.M. Van Wie, D.G. Drewry, Jr., D.E. King, and C.M. Hudson: The Hypersonic Environment: Required Operating Conditions and Design Challenges. *Journal of Materials Science*, 39, 5915 (2004).
39. T.A. Jackson, D.R. Eklund, and A.J. Fink: High Speed Propulsion: Performance Advantage of Advanced Materials. *Journal of Materials Science*, 39, 5905 (2004).
40. K.-I. Takagi: Development and Application of High Strength Ternary Boride Base Cermets. *Journal of Solid State Chemistry*, 179, 2809 (2006).
41. B. Yuan, G.-J. Zhang, Y.-M. Kan, and P.-L. Wang: Reactive Synthesis and Mechanical Properties of Mo₂NiB₂ Based Hard Alloy. *International Journal of Refractory Metals and Hard Materials*, 28, 291 (2010).
42. G.B. Raju and B. Basu: Development of High Temperature TiB₂-Based Ceramics. *Key Engineering Materials*, 395, 894 (2009).
43. B.R. Golla, T. Bhandari, A. Mukopadhyay, and B. Basu: Titanium Diboride. pp. 316-360 in Ultra-High Temperature Ceramics: Materials for Extreme Environment Applications, ed. by W.G. Fahrenholtz, E. Wuchina, W.E. Lee, and Y. Zhou, Wiley-Blackwell, New York, 2015.
44. A.K. Suri, N. Krishnamurthy, and I.S. Batra: Materials Issues in Fusion Reactors. *Journal of Physics: Conference Series*, 208, paper number 012001 (2010).
45. H.F. Jackson, D.D. Jayaseelan, W.E. Lee, M.J. Reese, F. Inam, D. Manara, C.P. Casoni, F. De Bruycker, and K. Boboridis: Laser Melting of Spark Plasma-Sintered Zirconium Carbide: Thermophysical Properties of a Generation IV Very High-Temperature Reactor Material. *International Journal of Applied Ceramic Technology*, 7, 316 (2010).
46. J. She, Y. Zhan, M. Pang, C. Li, and W. Yang: In-Situ Synthesized (ZrB₂+ZrC) Hybrid Short Fibers reinforced Zr Matrix Composites for Nuclear Applications. *International Journal of Refractory Metals and Hard Materials*, 29, 401 (2011).
47. E. Wuchina, E. Opila, M. Opeka, W. Fahrenholtz, and I. Talmy: UHTCs: Ultra-High Temperature Ceramic Materials for Extreme Environment Application. *Interface*, 16, 30 (2007).
48. M.M. Opeka, I.G. Talmy, and J.A. Zaykoski: Oxidation-Based Materials Selection for 2000°C+ Hypersonic Aerosurfaces: Theoretical Considerations and Historical Experience. *Journal of Materials Science*, 39, 5887 (2004).
49. T.H. Squire and J. Marschall: Material Property Requirements for Analysis and Design of UHTC Components in Hypersonic Applications. *Journal of the European Ceramic Society*, 30, 2239 (2010).
50. M.J. Gasch, D.T. Ellerby, and S.M. Johnson: Ultra-High Temperature Ceramic Composites. pp. 197- 224 in *Handbook of Ceramic Composites* ed. By N.P. Bansal, Kluwer Academic Publishers, Boston, 2005.
51. R. Telle, L.S. Sigl, and K. Takagi: Boride-Based Hard Materials. pp. 802-945 in *Handbook of Ceramic Hard Materials*, ed. by R. Riedel, Wiley-VCH, Weinheim, Germany (2000).
52. P.H. Mayrhofer, C. Mitterer, L. Hultman, and H. Clemens: Microstructural Design of Hard Coatings. *Progress in Materials Science*, 51, 1032 (2006).
53. Z. Xie, T. Zhou, and Y. Gou: Synthesis and Characterization of Zirconium Diboride Ceramic Precursor. *Ceramics International*, 41, 6226 (2015)

54. G.-J. Zhang, H.-T. Liu, W.-W. Wu, J. Zou, D.-W. Ni, W.-M. Guo, J.-X. Liu and X.-G. Wang: Reactive Processes for Diboride-Based Ultra-High Temperature Ceramics. pp. 33-59 in Ultra-High Temperature Ceramics: Materials for Extreme Environment Applications, ed. by W.G. Fahrenholtz, E. Wuchina, W.E. Lee, and Y. Zhou, Wiley-Blackwell, New York, 2015.
55. H. Moissan: Nouvelles Reserches sur le Chrome. *Comptes Rendus des Séances*, 119, 185 (1894).
56. H. Moissan; Reserches sur le tungsten. *Comptes Rendus des Séances*, 123, 13 (1896).
57. H. Moissan: Préparation et Propriétés du Titane. *Comptes Rendus des Séances*, 120, 290 (1895).
58. S.A. Tucker and H.R. Moody: The Preparation of a New Metal Boride. *Proceedings of the Chemical Society, London*, 17, 129 (1901).
59. S.A Tucker and H.R. Moody: The Preparation of Some New Metal Borides. *Journal of the Chemical Society*, 81, 14 (1902).
60. E. Wedekind: Synthese von Boriden im Elektrischen Vakuumofen. *Berichte der Deutschen Chemischen Gesellschaft*, 46, 1198 (1913).
61. P.M. McKenna: Tantalum Carbide: Its Relation to Other Hard Refractory Compounds. *Industrial and Engineering Chemistry*, 28, 767 (1936).
62. C. Agte and K. Moers: Methoden zur Reindarstellung hochschmelzender Carbide, Nitride und Boride und Beschreibung einiger ihrer Eigenschaften. *Zeitschrift für Anorganische und Allgemeine Chemie*, 198, 233 (1931).
63. D. Coster and G. Hervey: On the New Element Hafnium. *Nature*, 111, 185 (1923).
64. R. Kiessling: A Method for Preparing Boron of High Purity. *Acta Chemica Scandinavica*, 2, 707-712 (1948).
65. R. Kiessling: The Borides of Tantalum. *Acta Chemica Scandinavica*, 3, 603 (1949).
66. R. Kiessling: The Binary System Chromium-Boron. *Acta Chemica Scandinavica*, 3, 595 (1949).
67. R. Kiessling: The Crystal Structures of Molybdenum and Tungsten Borides. *Acta Chemica Scandinavica*, 1, 893 (1947).
68. R. Kiessling: The Binary System Zirconium-Boron. *Acta Chemica Scandinavica*, 3, 90 (1949).
69. P. Peshev, G. Bliznakov, and L. Leyarovska: On The Preparation of Some Chromium, Molybdenum, and Tungsten Borides. *Journal of Less Common Metals*, 13, 241 (1967).
70. P. Peshev and G. Bliznakov: On The Boro-thermic Preparation of Titanium, Zirconium, and Hafnium Borides. *Journal of Less Common Metals*, 14, 23 (1967).
71. P. Peshev, L. Leyarovska, and G. Bliznakov: On The Boro-thermic Preparation of Some Vanadium, Niobium, and Tantalum Borides. *Journal of Less Common Metals*, 15, 259 (1968).
72. G. Bliznakov and P. Peshev: A Thermodynamic Study of the Reactions in the Chemical Transport of Boron. *Journal of Less Common Metals*, 47, 61 (1976).
73. Y.B. Kuz'ma, T.I. Serebryakova, and A.M. Plakhina: Polymorphic Transformations of W_2B_5 . *Zhurnal Neorganicheskoi Khimii*, 12, 559 (1968).
74. J.A. Nelson, T.A. Willmore, and R.C. Womeldorph: Refractory Bodies Composed of Boron and Titanium Carbides Bonded with Metals. *Journal of the Electrochemical Society*, 98, 465 (1951).

75. G.A. Meerson, G.V. Samsonov, R.B. Kotel'nikov, and N.Y. Tsitina: Vacuum Thermal Production of Borides of Refractory Metals and Investigation of Several Boride Systems. *Sbornik Nauch Trudov Moskov. Univ. Tsvetnykh Metal. I Zolota*, 25, 209 (1955).
76. R. Meyer and H. Pastor: The Borides of Titanium and Zirconium Preparation, Properties, and Applications. *Bulletin de la Societe Francais de Ceramique*, 66, 59 (1965).
77. R. Thompson: The Chemistry of Metal Borides and Related Compounds. pp. 173-230 in *Progress in Boron Chemistry, Vol. 2*, ed. by R.J. Brotherson and H. Steinberg, Pergamon Press, Oxford, U.K., 1970.
78. L.Ya. Markovskii and N.V. Verkshina: A Magnesiumthermic Method for the Preparation of Metal Borides. *Zhurnal Prikladnoi Khimii*, 40, 1824 (1967).
79. J.L. Andrieux: Making Metallic Powders by Electrolysis of Fused Salts. *Revue de Metallurgie*, 45, 49 (1948).
80. J.T. Norton, H. Blumenthal, and S.J. Sindeland: Structure of Diborides of Titanium, Zirconium, Columbium, Tantalum and Vanadium. *Metals Transactions*, 185, 749 (1949).
81. C. Agte and K. Moers: Methoden zur Reindarstellung hochschmelzender Carbide, Nitride und Boride und Beschreibung einiger ihrer Eigenschaften. *Zeitschrift für Anorganische und Allgemeine Chemie*, 198, 233 (1931).
82. A. Roos: Boron Derivatives, Metallic Borides, and Their Uses. *Chimie et Industrie*, 82, 339 (1959).
83. J.J. Gebhardt and R.F. Cree: Vapor-Deposited Borides of Group IVA Metals. *Journal of the American Ceramic Society*, 48, 262 (1965).
84. R.H. Valentine, T.F. Jambois, and J.L. Margrave: Thermodynamic Properties of Inorganic Substances VII: The High Temperature Heat Content of Zirconium Diboride. *Journal of Chemical and Engineering Data*, 9, 182 (1964).
85. D. Kalish and E.V. Clougherty: Densification Mechanisms in High-Pressure Hot-Pressing of HfB_2 . *Journal of the American Ceramic Society*, 52, 26 (1969).
86. D. Kalish, E.V. Clougherty, and K. Kreder: Strength, Fracture Mode, and Thermal Stress Resistance of HfB_2 and ZrB_2 . *Journal of the American Ceramic Society*, 52, 30 (1969).
87. E. Rudy, St. Windisch, and Y.A. Chang: Ternary Phase Equilibria in Transition Metal-Boron-Carbon-Silicon Systems: Part I. Related Binary Systems, Volume I. Mo-C System. *Technical Report Number AFML-TR-65-2*, Air Force Materials Laboratory, Wright-Patterson Air Force Base, January 1965.
88. R. Naslain, J. Etourneau, and P. Hagenmuller: Alkali Metal Borides. pp. 262-292 in *Boron and Refractory Borides*, ed. by V.I. Markovich, Springer-Verlag, Berlin (1977).
89. R. Naslain, A. Guette, and P. Hagenmuller: Crystal Chemistry of Some Boron-Rich Phases. *Journal of Less Common Metals*, 47, 1 (1976).
90. J. Etourneau, J.P. Mercurio, R. Naslain, and P. Hagenmuller: Comparative Study of the Thermal Stability of Some Rare-Earth Borides. *Comptes Rendus des Seances de l'Academie des Sciences, Serie C: Sciences Chimiques*, 274, 1688 (1972).
91. G.V. Samsonov and V.S. Nespor: Alloys of Rare Metals with Boron and Silicon for Some Radio- and Electrotechnical Application. *Redkie Metally I Splavy, Trudy Pervogo Vseoyuz. Soveshchaniya po Splavam Redkikh Metal.*, Akad. Nauk S.S.S.R., Inst. Met. Im. A.A. Baikova, Moscow, 392 (1957).
92. P. Rogl and H. Nowotny: Structural Chemistry of Ternary Metal Borides: Rare Earth Metal-Noble Metal-Boron. *Rare Earths in Modern Science and Technology*, 2, 173 (1980).

93. P. Rogl and H. Nowotny: Structural Chemistry of Ternary Metal Borides. *Journal of Less Common Metals*, 61, 39 (1978).
94. R. Thomson: Production, Fabrication, and Uses of Borides. pp. 113-120 in *The Physics and Chemistry of Carbides, Nitrides and Borides*, ed. by R. Freer, Kluwer Academic Publishers, Dordrecht (1990).
95. T. Lundström: Transition Metal Borides. pp. 351-376 in *Boron and Refractory Borides*, ed. by V.I. Markovich, Springer-Verlag, Berlin (1977).
96. C. Mroz: Zirconium Diboride. *American Ceramic Society Bulletin*, 73, 141 (1994).
97. J.J. Kim and C.H. McMurtry: Titanium Diboride Powder Production for Engineered Ceramics. *Ceramic Engineering and Science Proceedings*, 6, 1313 (1985).
98. P. Schwarzkopf and R. Kieffer, Refractory Hard Metals: Borides, Carbides, Nitrides, and Silicides, Ch. 6: Zirconium Carbide, The MacMillan Company, New York (1953).
99. G.J.K. Harrington, J. Lonergan, W.G. Fahrenholtz, and G.E. Hilmas: Processing for Improved Thermal Conductivity of Zirconium Diboride. 12th International Conference on Ceramic Processing Science (ICCPs-12), Portland, OR, August 4-7, 2013.
100. "Hafnium," p B-19 in CRC Handbook of Chemistry and Physics, 62nd Edition, ed. by R.C. Weast and M.J. Astle, CRC Press, Inc., Boca Raton, FL, 1983.
101. J.M. Lonergan, W.G. Fahrenholtz, and G.E. Hilmas: Thermal Properties of Hf-Doped ZrB₂ Ceramics. *Journal of the American Ceramic Society*, 98, 2689 (2015).
102. J.M. Lonergan, W.G. Fahrenholtz, and G.E. Hilmas: Zirconium Diboride with High Thermal Conductivity. *Journal of the American Ceramic Society*, 97, 1689 (2014).
103. H. Zhao, Y. He, and Z.Z. Jin: Preparation of Zirconium Diboride Powder. *Journal of the American Ceramic Society*, 78, 2534 (1995).
104. S. Baik and P. F. Becher: Effect of Oxygen Contamination on Densification of TiB₂. *Journal of the American Ceramic Society*, 70, 527 (1987)
105. A.L. Chamberlain, W.G. Fahrenholtz, and G.E. Hilmas: Pressureless Sintering of Zirconium Diboride. *Journal of the American Ceramic Society*, 89 450 (2006).
106. S. Zhu, W.G. Fahrenholtz, G.E. Hilmas, and S.C. Zhang: Pressureless Sintering of Carbon-Coated Zirconium Diboride Powders. *Materials Science and Engineering A*, 459, 167 (2007).
107. S.C. Zhang, G.E. Hilmas, and W.G. Fahrenholtz: Pressureless Densification of Zirconium Diboride with Boron Carbide Additions. *Journal of the American Ceramic Society*, 89, 1544 (2006).
108. W.G. Fahrenholtz, G.E. Hilmas, S.C. Zhang, and S. Zhu: Pressureless Sintering of Zirconium Diboride: Particle Size and Additive Effects. *Journal of the American Ceramic Society*, 91, 1398 (2008).
109. G. van de Goor, P. Sagesser, and K. Berroth: Electrically Conductive Ceramic Composites. *Solid State Ionics*, 101-103, 1163 (1997).
110. L. H. Li, H. E. Kim, and E. S. Kang: Sintering and Mechanical Properties of Titanium Diboride with Aluminum Nitride as a Sintering Aid. *Journal of the European Ceramic Society*, 22, 973 (2002)
111. F. Monteverde and A. Bellosi, "Beneficial Effect of AlN as Sintering Aid on Microstructure and Mechanical Properties of Hot-Pressed ZrB₂," *Advanced Engineering Materials*, 5(7) 508-512 (2003).

112. S. Zhu, W.G. Fahrenholtz, G.E. Hilmas, and S.C. Zhang: Pressureless Sintering of Zirconium Diboride Using Boron Carbide and Carbon Additions. *Journal of the American Ceramic Society*, 90, 3660 (2007).
113. D. Sciti, L. Silvestroni, V. Medri, and F. Monteverde: Sintering and Densification Mechanisms of Ultra-High Temperature Ceramics. pp. 112-143 in *Ultra-High Temperature Ceramics: Materials for Extreme Environment Applications*, ed. by W.G. Fahrenholtz, E.J. Wuchina, W.E. Lee, and Y. Zhou, Wiley-Blackwell, New York, 2014.
114. W.-M. Guo, Z.-G. Yang, and G.-J. Zhang: Synthesis of submicrometer HfB₂ powder and its densification. *Mater. Lett.* **83**, 52 (2012).
115. X-G. Wang, W-M. Guo and G-J. Zhang: Pressureless sintering mechanism and microstructure of ZrB₂-SiC ceramics doped with boron. *Scr. Mater.* **61**, 177 (2009).
116. S. Ran, O. Van der Biest and J. Vleugels: ZrB₂ powders synthesis by borothermal reduction. *J. Am. Ceram. Soc.* **93**, 1586 (2010).
117. J. K. Sonber, T. S. R. C. Murthy, C. Subramanian, S. Kumar, R. K. Fotedar and A. K. Suri: Investigations on synthesis of ZrB₂ and development of new composites with HfB₂ and TiSi₂. *Int. J. Refract. Met. Hard Mater.*, **29**, 21 (2011).
118. G.J. Zhang, Z.Y. Deng, N. Kondo, J. F. Yang and T. Ohji: Reactive Hot Pressing of ZrB₂-SiC Composites. *J. Am. Ceram. Soc.*, 83, 2330 (2000)
119. G.J. Zhang, M. Ando, J.F. Yang, T. Ohji, S. Kanzaki: Boron carbide and nitride as reactants for in situ synthesis of boride-containing ceramic composites. *Journal of the European Ceramic Society*, 24, 171 (2004)
120. J. Zou, J. Liu, G.-J. Zhang, S. Huang, J. Vleugels, O. Van der Biest and J.Z. Shen: Hexagonal BN-encapsulated ZrB₂ particle by nitride boronizing. *Acta Materialia*, 72, 167 (2014)
121. W.G. Fahrenholtz: Reactive Processing in Ceramic-Based Systems. *International Journal of Applied Ceramic Technology*, 3, 1 (2006).
122. Y.M. Chiang, J.S. Haggerty, R.P. Messner and C. Demetry: Reaction-based processing Methods for ceramic-matrix. *American Ceramic Society Bulletin*, 68, 420 (1989).
123. A.L. Chamberlain, W.G. Fahrenholtz, and G.E. Hilmas: Reactive Processing of Zirconium Diboride. *Journal of the European Ceramic Society*, 29, 3401 (2009).
124. W.-W. Wu, G.-J. Zhang and Y. Sakka: Nanocrystalline ZrB₂ powders prepared by mechanical alloying. *Journal of Asian Ceramic Societies*, 1, 304 (2013).
125. D. Lee, J.J. Vlassak, and K. Zhao: First-Principles Theoretical Studies and Nanocalorimetry Experiments on Solid-State Alloying of Zr-B. *Nano Letters*, 15, 6553 (2015)
126. A.L. Chamberlain, W.G. Fahrenholtz and G.E. Hilmas: Low Temperature Densification of Zirconium Diboride Ceramics by Reactive Hot Pressing. *Journal of the American Ceramic Society*, 89, 3638 (2006).
127. C. Hu, J. Zou, Q. Huang, G. Zhang, S. Guo, and Y. Sakka: Synthesis of Plate-Like ZrB₂ Grains. *J. Am. Ceram. Soc.*, 95, 85 (2012)
128. H.J. Jung, Y. Sohn, H.G. Sung, H.S. Hyun and W.G. Shin: Physicochemical properties of ball milled boron particles: Dry vs. wet ball milling process. *Powder Technology*, 269, 548 (2015).
129. W.G. Fahrenholtz: Reactive Hot Pressing of Al₂O₃-Ni Composites. *Journal of Materials Science*, 38, 3073 (2003).
130. S. Guo, C. Hu and Y. Kagawa: Mechanochemical Processing of Nanocrystalline Zirconium Diboride Powder. *J. Am. Ceram. Soc.*, 94, 3643 (2011).

131. S. Ran, O. Van der Biest, and J. Vleugels: ZrB₂–SiC Composites Prepared by Reactive Pulsed Electric Current Sintering. *J. Euro. Ceram. Soc.*, 30, 2633 (2010)
132. S. Guo, D.H. Ping and Y. Kagawa: Synthesis of zirconium diboride platelets from mechanically activated ZrCl₄ and B powder mixture. *Ceramics International*, 38, 5195 (2012)
133. I. Parkin: Solid State Metathesis Reaction For Metal Borides, Silicides, Pnictides and Chalcogenides: Ionic or Elemental Pathways. *Chem. Soc. Reviews*, 25, 199 (1996).
134. L. Rao, E.G. Gillan and R.B. Kanera: Rapid synthesis of transition-metal borides by solid-state metathesis. *Journal of Material Research*, 10, 353(1995).
135. E.G. Gillan and R.B. Kaner: Synthesis of Refractory Ceramics via Rapid Metathesis Reactions between Solid-State Precursors. *Chemistry of Materials*, 8, 333 (1996)
136. R. Licheri, R. Orrù, C.a Musa, and G. Cao: Combination of SHS and SPS Techniques for fabrication of fully dense ZrB₂–ZrC–SiC composites. *Materials Letters*, 62, 432 (2008)
137. W.-W. Wu, Z. Wang, G.-J. Zhang, Y.-M. Kan and P.-L. Wang: ZrB₂ MoSi₂ composites toughened by elongated ZrB₂ grains via reactive hot pressing. *Scripta Materialia*, 61, 316 (2009).
138. H.-T. Liu, W.-W Wu, J. Zou, D.-W. Ni, Y.-M. Kan and G.-J. Zhang: In situ synthesis of ZrB₂–MoSi₂ platelet composites: Reactive hot pressing process, microstructure and mechanical properties. *Ceramics International*, 38, 4751 (2012)
139. H.L. Zhao, J.L. Wang, Z.M. Zhu, J. Wang, W. Pan: Mechanical properties and microstructure of in situ synthesized ZrB₂–ZrN_{1-x} composites. *Journal of Materials Science* 41, 1769 (2006).
140. H. Zhao, J. Wang, Z. Zhu, W. Pan and J. Wang: In situ synthesis mechanism of ZrB₂–ZrN composite. *Materials Science and Engineering A*, 452–453, 130 (2007).
141. W.-W. Wu, M. Estili, T. Nishimura, G.-J. Zhang and Y. Sakka: Machinable ZrB₂–SiC–BN composites fabricated by reactive spark plasma sintering. *Materials Science & Engineering A* 582, 41 (2013)
142. E. Breval and W.B. Johnson: Microstructure of Platelet-Reinforced Ceramics Prepared by the Directed Reaction of Zirconium with Boron Carbide. *J Am Ceram Soc.*, 75, 2139 (1992).
143. W.-W. Wu, G.-J. Zhang, Y.M. Kan, and Y. Sakka: Synthesis, microstructure and mechanical properties of reactively sintered ZrB₂–SiC–ZrN composites. *Ceramics International*, 39, 7273 (2013).
144. Q. Qu, J. Han, W. Han, X. Zhang, and C. Hong: In situ synthesis mechanism and characterization of ZrB₂–ZrC–SiC ultra high-temperature ceramics. *Materials Chemistry and Physics*, 110, 216 (2008).
145. J.W. Zimmermann, G.E. Hilmas, W.G. Fahrenholtz, F. Monteverde, and A. Bellosi: Fabrication and Properties of Reactively Hot Pressed ZrB₂–SiC Ceramics. *Journal of the European Ceramic Society*, 27, 2729 (2007).
146. L. Rangaraj, C. Divakar, and V. Jayaram: Fabrication and Mechanisms of Densification of ZrB₂-Based Ultra-High Temperature Ceramics by Reactive Hot Pressing. *Journal of the European Ceramic Society*, 30, 129 (2010).
147. Y. Zhao, L.-J. Wang, G.-J. Zhang, W. Jiang, and L.-D. Chen: Preparation and Microstructure of a ZrB₂–SiC Composite Fabricated by the Spark Plasma Sintering-Reactive Synthesis Method. *Journal of the American Ceramic Society*, 90, 4040 (2007).

148. W.W. Wu, G.J. Zhang, Y.M. Kan, P.L. Wang: Reactive hot pressing of $\text{ZrB}_2\text{-SiC-ZrC}$ ultra high-temperature ceramics at 1800 degrees C. *Journal of the American Ceramic Society*, 89, 2967 (2006).
149. F. Monteverde: Progress in the Fabrication of Ultra-High-Temperature Ceramics: In Situ Synthesis, Microstructure and Properties of a Reactive Hot Pressed $\text{HfB}_2\text{-SiC}$. *Composites Science and Technology*, 65, 1869 (2005).
150. W.W. Wu, G.-J. Zhang, Y.M. Kan, and P.-L. Wang PL: Reactive hot pressing of $\text{ZrB}_2\text{-SiC-ZrC}$ composites at 1600 °C. *J Am Ceram Soc.*, 91, 2501 (2000).
151. W.-W. Wu, G.-J. Zhang, Y.-M. Kan and P.-L. Wang: Combustion synthesis of $\text{ZrB}_2\text{-SiC}$ composite powders ignited in air. *Materials Letters*, 63, 1422 (2009)
152. T. Tsuchida and S. Yamamoto: Mechanical activation assisted self-propagating high-Temperature synthesis of ZrC and ZrB_2 in air from Zr/B/C powder mixtures. *Journal of the European Ceramic Society*, 24, 45 (2004)
153. T. Tsuchida and S. Yamamoto: MA-SHS and SPS of $\text{ZrB}_2\text{-ZrC}$ composites. *Solid State Ionics*, 172, 215 (2004)
154. W.-W. Wu, W.-L. Xiao, M. Estili, G.-J. Zhang and Y. Sakka: Microstructure and mechanical properties of $\text{ZrB}_2\text{-SiC-BN}$ composites fabricated by reactive hot pressing and reactive spark plasma sintering. *Scripta Materialia*, 68, 889 (2013)
155. J. Zou, S.G. Huang, K. Vanmeensel, G.J. Zhang, J. Vleugels and O. Van der Biest: Spark Plasma Sintering of Superhard $\text{B}_4\text{C-ZrB}_2$ Ceramics by Carbide Boronizing. *J. Am. Ceram. Soc.*, 96, 1055 (2013).
156. J. Zou, J. Liu, J. Zhao, G.-J. Zhang, S. Huang, B. Qian, J. Vleugels, O. Van der Biest, J.Z. Shen: A top-down approach to densify $\text{ZrB}_2\text{-SiC-BN}$ composites with deeper homogeneity and improved reliability. *Chemical Engineering Journal*, 249, 93 (2014).
157. D. Wang, S. Ran, L. Shen, H. Sun, and Q. Huang: Fast synthesis of $\text{B}_4\text{C-TiB}_2$ composite powders by pulsed electric current heating TiC-B mixture. *Journal of the European Ceramic Society*, 35, 1107 (2015)
158. D. Vallauri, I.C. At'ias Adrian, and A. Chrysanthou: TiC-TiB_2 composites: A review of phase relationships, processing and properties. *Journal of the European Ceramic Society*, 28, 1697 (2008)
159. N. J. Welham: Formation of nanometric TiB_2 from TiO_2 . *J. Am. Ceram. Soc.* **83**, 1290 (2000).
160. N. Setoudeh and N. J. Welham: Formation of zirconium diboride by room temperature mechanochemical reaction between ZrO_2 , B_2O_3 and Mg. *J. Alloys & Compounds* **420**, 225 (2006).
161. R. Ricceri and P. Matteazzi: A fast and low-cost room temperature process for TiB_2 formation by mechanosynthesis. *Mater. Sci. & Eng. A*, **379**, 341 (2004).
162. D. L. Segal: Chemical routes for the preparation of powders. *Phys. Chem. Carbides, Nitrides Borides*, **185**, 3 (1990).
163. Y. D. Blum and H-J. Kleebe: Chemical reactivities of hafnium and its derived boride, carbide and nitride compounds at relatively mild temperature. *J. Mater. Sci.*, **39**, 6023 (2004).
164. H. R. Hoekstra and J. J. Katz: The preparation and properties of the group IV-B metal borohydrides. *J. Am. Chem. Soc.* **71**, 2488 (1949).

165. W. E. Reid, J. M. Bish and A. Brenner: Electrodeposition of metals from organic solutions. III. Preparation and electrolysis of titanium and zirconium compounds in non-aqueous media. *J. Electrochem. Soc.*, **104**, 21 (1957).
166. M. K. Gallagher, W. E. Rhine and H. K. Bowen: Low-temperature route to high-purity titanium, zirconium and hafnium diboride powders and films. in J.D. Mackenzie and D.R. Ulrich (eds.), *Ultrastructure Processing of Advanced Ceramics*, Wiley Interscience, New York, pp. 901–906 (1988).
167. L. Chen, Y. Gu, Z. Yang and Y. Qian: Preparation and some properties of nanocrystalline ZrB_2 powder. *Scripta Materialia* **50**, 959 (2004).
168. L. Chen, Y. Gu, L. Shi, Z. Yang, J. Ma and Y. Qian: Synthesis and oxidation of nanocrystalline HfB_2 . *J. Alloys & Compounds* **368**, 353 (2004).
169. Y. Yan, Z. Huang, S. Dong, and D. Jiang: New route to synthesize ultra-fine zirconium diboride powders using inorganic-organic hybrid precursors. *J. Am. Ceram. Soc.* **89**, 3589 (2006).
170. Y. J. Yan, Z. R. Huang, S. M. Dong, and D. L. Jiang: Carbothermal preparation of ultra-fine TiB_2 powders using solution-derived precursors via sol-gel method. *Key Eng. Mater.* **336-338**, 944 (2007).
171. S. Venugopal, A. Paul, B. Vaidhyanathan, J. G. P. Binner, E.E. Boakye, K. Keller, P. Mogilevsky, A. Katz and P. M. Brown: Sol-gel synthesis and formation mechanism of ultra-high temperature ceramic: HfB_2 . *J. Am. Cer. Soc.* **97**, 92 (2014).
172. S. Venugopal, D. D. Jayaseelan, A. Paul, B. Vaidhyanathan, J. G.P. Binner, P. M. Brown: Screw Dislocation Assisted Spontaneous Growth of HfB_2 Tubes and Rods. *J. Am. Ceram. Soc.* **98**, 2060 (2015).
173. S. Venugopal, A. Paul, B. Vaidhyanathan, J. G. P. Binner, A. Heaton, P. M. Brown: L Synthesis and spark plasma sintering of sub-micron HfB_2 : Effect of various carbon sources. *J. Eur. Ceram. Soc.* **34**, 1471 (2014).
174. Y. Cao, H. Zhang, F. Li, L. Lu and S. Zhang: Preparation and characterization of ultrafine ZrB_2 -SiC composite powders by a combined sol-gel and microwave boro/carbothermal reduction method. *Ceram. Int.* **41**, 7823 (2015).
175. Y. Xie, T. H. Sanders, and R. F. Speyer: Solution-based synthesis of submicrometer ZrB_2 and ZrB_2 - TaB_2 . *J. Am. Ceram. Soc.* **91**, 1469 (2008).
176. D. L. Hu, Q. Zheng, H. Gu, D. W. Ni, and G. J. Zhang: Role of WC additive on reaction, solid-solution and densification in HfB_2 -SiC ceramics. *J. Eur. Ceram. Soc.* **34**, 611 (2014).
177. X. H. Zhang, P. Hu, J. C. Han, L. Xu, and S. H. Meng: The addition of lanthanum hexaboride to zirconium diboride for improved oxidation resistance. *Scr. Mater.* **57** 1036 (2007).
178. S. R. Levine and E. J. Opila: Tantalum addition to zirconium diboride for improved oxidation resistance. *Nasa/TM-2003-212483*, 1 (2003).
179. F. Monteverde: Ultra-high temperature HfB_2 -SiC ceramics consolidated by hot-pressing and spark plasma sintering. *J. Alloys Compd.* **428**, 197 (2007).
180. Y. Wang, L. Luo, J. Sun and L. An: ZrB_2 -SiC(Al) ceramics with high resistance to oxidation at 1500°C. *Corros. Sci.* **74**, 154 (2013).
181. J. Han, P. Hu, X. Zhang, S. Meng, and W. Han: Oxidation-resistant ZrB_2 -SiC composites at 2200°C. *Compos. Sci. Technol.* **68**, 799 (2008).

182. P.A. Williams, R. Sakidja, J. H. Perepezko and P. Ritt: Oxidation of ZrB₂-SiC ultra-high temperature composites over a wide range of SiC content. *J. Eur. Ceram. Soc.* **32**, 3875 (2012).
183. W. G. Fahrenholtz and G. E. Hilmas: Oxidation of ultra-high temperature transition metal diboride ceramics. *Int. Mater. Rev.* **57**, 61 (2012).
184. D-W. Ni, G-J. Zhang, Y-M. Kan, and P-L. Wang: Synthesis of monodispersed fine hafnium diboride powders using carbo/borothermal reduction of hafnium dioxide. *J. Am. Ceram. Soc.* **91**, 2709 (2008).
185. E. Opila and M. Halbig: Oxidation of ZrB₂-SiC. *Cer. Eng. Sci. Proc.* **22**, 221 (2008).
186. B. Zhao, Y. Zhang, J. Li, B. Yang, T. Wang, Y. Hu, D. Sun, R. Li, S. Yin, Z. Feng and T. Sato: Morphology and mechanism study for the synthesis of ZrB₂-SiC powders by different methods. *J. Solid State Chem.* **207**, 1 (2013).
187. M. A. Avilés, J. M. Córdoba, M. J. Sayagués, M. D. Alcalá and F. J. Gotor: Mechanosynthesis of Hf_{1-x}Zr_xB₂ Solid Solution and Hf_{1-x}Zr_xB₂/SiC Composite Powders. *J. Am. Ceram. Soc.* **93**, 696 (2010).
188. D. L. McClane, W. G. Fahrenholtz and G. E. Hilmas: Thermal properties of (Zr,TM)B₂ solid solutions with TM = Ta, Mo, Re, V and Cr. *J. Am. Ceram. Soc.* **98**, 637 (2015).
189. D. L. McClane, W. G. Fahrenholtz and G. E. Hilmas: Thermal properties of (Zr,TM)B₂ solid solutions with TM = Hf, Nb, W, Ti and Y. *J. Am. Ceram. Soc.* **97**, 1552 (2014).
190. B. Post, F.W.Glaser and D. Moskowitz: Transition Metal Diborides. *Acta Metall.* **2**, 20 (1954).
191. S. Otani, T. Aizawa and N. Kieda: Solid solution ranges of zirconium diboride with other refractory diborides: HfB₂, TiB₂, TaB₂, NbB₂, VB₂ and CrB₂. *J. Alloys Compd.* **475**, 273 (2009).
192. W. G. Fahrenholtz, G. E. Hilmas, I. G. Talmy and J. A. Zaykoski: Refractory diborides of zirconium and hafnium. *J. Am. Ceram. Soc.* **90**, 1347 (2007).
193. Y. Jiang, R. Li, Y. Zhang, B. Zhao, J. Li and Z. Feng: Tungsten doped ZrB₂ powder synthesized synergistically by co-precipitation and solid-state reaction methods. *Procedia Eng.* **27**, 1679 (2012).
194. I. G. Talmy, J. a Zaykoski and M. M. Opeka: High-temperature chemistry and oxidation of ZrB₂ ceramics containing SiC, Si₃N₄, Ta₅Si₃ and TaSi₂. *J. Am. Ceram. Soc.* **91**, 2250 (2008).
195. D. Sciti, V. Medri and L. Silvestroni: Oxidation behaviour of HfB₂-15 vol.% TaSi₂ at low, intermediate and high temperatures. *Scr. Mater.* **63**, 601 (2010).
196. S. C. Zhang, G. E. Hilmas and W. G. Fahrenholtz: Improved oxidation resistance of zirconium diboride by tungsten carbide additions. *J. Am. Ceram. Soc.* **91**, 3530 (2008).
197. S. C. Zhang, G. E. Hilmas and W. G. Fahrenholtz: Oxidation of zirconium diboride with tungsten carbide additions. *J. Am. Ceram. Soc.* **94**, 1198 (2011).
198. R. He, X. Zhang, W. Han, P. Hu and C. Hong: Effects of solids loading on microstructure and mechanical properties of HfB₂-20 vol.% MoSi₂ ultra high temperature ceramic composites through aqueous gelcasting route. *Mater. Des.* **47**, 35 (2013).

List of Tables

Table I. Summary of composition, crystal structure, and properties of selected transition metal boride compounds.

Table II. Example synthesis reactions for transition metal (TM) diborides.

Table III. Synthesis reactions, $\Delta G_{\text{rxn}}^{\circ}$ at 300 K, and reaction conditions for the formation of ZrB₂-containing ceramics by displacement reactions using Zr as a precursor.

Tables

Table I. Summary of composition, crystal structure, and properties of selected transition metal boride compounds.

Metal	Boride Compounds	Melting Temperature (°C) ¹	Structure Type	Space Group ²	Density (g/cm ³) ²	Hardness (GPa)/ Load (N)	Elastic Modulus (GPa)
Ti	TiB	~2200	FeB	Pnma	4.58	18.6/9.8 ³	427 ⁵
	Ti ₃ B ₄	~2200	-	Immm	4.56	33.1/* ⁴	554 ⁴
	TiB ₂	3225	AlB ₂	P6/mmm	4.51	35/9.8 ³¹	560 ³¹
Zr	ZrB ₂	3250	AlB ₂	P6/mmm	6.09	23/9.8 ⁶	526 ⁷
Hf	HfB ¹	2100	FeB	Pnma	12.19	-	-
	HfB ₂	3380	AlB ₂	P6/mmm	11.212	28/* ²⁵	480 ³⁵
Nb	NbB ₂	2990	AlB ₂	P6/mmm	6.97	18.0/9.8 ¹⁰	505 ²³
Mo	Mo ₂ B	2290	Al ₂ Cu	I4/mcm	9.23	18.9/* ¹¹	389 ¹¹
	MoB	2600	-	I4 ₁ /amd	8.67	21.3/* ¹¹	496 ¹¹
	M.oB ₂	2375	AlB ₂	P6/mmm	7.87	24.4/* ¹¹	569 ¹¹
	Mo ₂ B ₅	2140	-	R $\bar{3}$ m	6.80	22.8/* ¹¹	554 ¹¹
Ta	TaB	3090	NiAs	P6 ₃ /mmc	14.20	28.6/* ¹²	420 ¹⁴
	TaB ₂	3037	AlB ₂	P6/mmm	12.6	25.6/9.8 ¹³	555 ¹³
W	W ₂ B	2670 ¹⁵	Al ₂ Cu	I4/mcm	17.09	-	441 ¹⁷
	WB	2665 ¹⁵	-	I4 ₁ /amd	15.74	28.9/?? ¹⁶	489 ¹⁸
	WB ₂	-	ReB ₂	P6 ₃ /mmc	12.76	-	-
	W ₂ B ₅	2365 ¹⁵	ReB ₂	P6 ₃ /mmc	11.19	-	37 ¹⁷
Re	ReB ₂	2400	ReB ₂	P6 ₃ /mmc	12.7	18/4.9 ¹⁹	382 ¹⁹
Os	OsB ₂	1870 ²⁰	RuB ₂	Pmmn	12.83	20/2.0 ²¹	410 ²¹

* Calculated value and ?? indicates not stated in the reference

¹ HfB is shown on phase diagrams including those by Rogl [8] and Rudy [9], but no property data or reports of synthesis were found for this compound.

Table II. Example synthesis reactions for transition metal (TM) diborides.

Reaction	
$\text{TMO}_{2(s)} + \text{B}_2\text{O}_{3(l)} + 5\text{C}_{(s)} \rightarrow \text{TMB}_{2(s)} + 5\text{CO}_{(g)}$	1
$\text{TM}_{(s)} + 2\text{B}_{(s)} \rightarrow \text{TMB}_{2(s)}$	2
$3\text{TMO}_{2(s)} + 10\text{B}_{(s)} \rightarrow 3\text{TMB}_{2(s)} + 2\text{B}_2\text{O}_{3(l)}$	3
$2\text{TMO}_{2(s)} + \text{B}_4\text{C}_{(s)} + 3\text{C}_{(s)} \rightarrow 2\text{TMB}_{2(s)} + 4\text{CO}_{(g)}$	4
$7\text{TMO}_{2(s)} + 5\text{B}_4\text{C}_{(s)} \rightarrow 7\text{ZrB}_{2(s)} + 3\text{B}_2\text{O}_{3(l)} + 5\text{CO}_{(g)}$	5
$3\text{TMO}_{2(s)} + 10\text{Al}_{(l)} + 3\text{B}_2\text{O}_{3(l)} \rightarrow 3\text{TMB}_{2(s)} + 5\text{Al}_2\text{O}_{3(s)}$	6
$\text{TMO}_{2(s)} + 5\text{Mg}_{(l)} + \text{B}_2\text{O}_{3(l)} \rightarrow \text{TMB}_{2(s)} + 5\text{MgO}_{(s)}$	7
$\text{TMO}_{2(s)} + \text{B}_2\text{O}_{3(s)} \xrightarrow{\text{CaO}+\text{CaF}_2} \text{TMB}_{2(s)} + \frac{5}{2}\text{O}_{2(g)}$	8
$\text{TMCl}_{4(g)} + 2\text{BCl}_{2(g)} + 5\text{H}_{2(g)} \rightarrow \text{TMB}_{2(s)} + 10\text{HCl}_{(g)}$	9

Table III. Synthesis reactions, $\Delta G_{\text{rxn}}^{\circ}$ at 300 K, and reaction conditions for the formation of ZrB₂-containing ceramics by displacement reactions using Zr as a precursor.

	Reaction	$\Delta G_{\text{rxn},300\text{K}}^{\circ}$ (kJ)	Reaction Conditions	References
14	$2\text{Zr} + \text{Si} + \text{B}_4\text{C} \rightarrow 2\text{ZrB}_2 + \text{SiC}$	-644	<1500°C in Ar	118, 145
15	$(2 + x)\text{Zr} + (1 - x)\text{Si} + \text{B}_4\text{C} \rightarrow \text{ZrB}_2 + (1 - x)\text{SiC} + x\text{ZrC}$	-657 at x = 0.1	<1500°C in Ar	148, 144
16	$8\text{Zr} + 1.5\text{Si} + 2\text{B}_4\text{C} + 3.5\text{C} \rightarrow 4\text{ZrB}_2 + 1.5\text{SiC} + 4\text{ZrC}$	-2027	SHS	136
17	$\text{Zr} + 2\text{Si} + \text{Mo} + 2\text{B} \rightarrow \text{ZrB}_2 + \text{MoSi}_2$	-437	~1000°C in Ar	137, 138
18	$3\text{Zr} + 2\text{BN} \rightarrow \text{ZrB}_2 + 2\text{ZrN}$ (ZrN _{1-x} with 0 < x < 1)	-542	~1600°C in Ar	139, 140
19	$4\text{Zr} + \text{Si}_3\text{N}_4 + 3\text{B}_4\text{C} \rightarrow 4\text{ZrB}_2 + 3\text{SiC} + 4\text{BN}$	-1478	1200°C, vacuum	141
20	$3\text{Zr} + \text{B}_4\text{C} \rightarrow 2\text{ZrB}_2 + \text{ZrC}$ (ZrC _{1-x} with 0 < x < 1)	-768	<800°C	148, 142
21	$10\text{Zr} + \text{Si}_3\text{N}_4 + 3\text{B}_4\text{C} \rightarrow 6\text{ZrB}_2 + 3\text{SiC} + 4\text{ZrN}$	-2562	<1800°C	143

List of Figures

- Figure 1.** Standard state Gibbs' free energy of formation as a function of temperature for the synthesis of ZrB_2 from [103]
- Figure 2.** Schematic illustrating reactions responsible for removal of oxygen impurities from the surface of ZrB_2 particles [106].
- Figure 3.** Cross section of the reaction front for boron (black at top of image) reacting with zirconium (white at bottom of image) to form ZrB_2 (gray in the middle of the image) from [123].
- Figure 4.** Morphology of ZrB_2 powders synthesized from (a) attrition milled Zr-B mixtures followed by heat treatment at 600 °C for 6h,¹²⁴ (b) attrition milled Zr-B mixtures followed by heat treatment at 1650°C for 1h,¹²⁴ (c) mixed of Zr, B, Si, and W powders heat treated at 1550°C for 30min in argon,¹²⁷ and (d) and (e) mixed ZrH_2 and B heated to 900°C.¹²⁴
- Figure 5.** Morphologies for starting (a) Si, (b) ZrN , and (c) B_4C powders and the resulting ZrB_2 -SiC-hBN materials shown in (d) secondary electron and (e) scattering modes showing significant reduction in particle size after synthesis.¹⁵⁶
- Figure 6.** Chemical reactivities of Hf and Hf-based compounds. Reactions with reagents marked in bold letters proceed (at least partially) at 1500°C or below. The rest require higher temperatures, e.g., borothermal, carbothermal, and carbo/borothermal reduction reactions. Additional reaction products within each of the reactions (if present) are omitted. Diagram based on Figure 14 in Reference 163.
- Figure 7.** SEM image of a ZrB_2 powder synthesized by a sol gel route involving carbothermal reduction at 1500°C for 1 h [169].
- Figure 8.** TEM images of the carbon structures (left) resulting from the pyrolysis of different carbon sources at 1000°C for 0.1 h and the corresponding FEGSEM images of the resultant HfB_2 powders after heat treatment at 1600°C for 2 h using (a) pitch, (b) sucrose, (c) graphite, (d) C-Black N115, (e) C-Black N772 and (f) MWCNT [173].
- Figure 9.** Schematic of the phase evolution in the powders prepared via sol-gel and microwave boro/carbothermal reduction process.¹⁷⁴

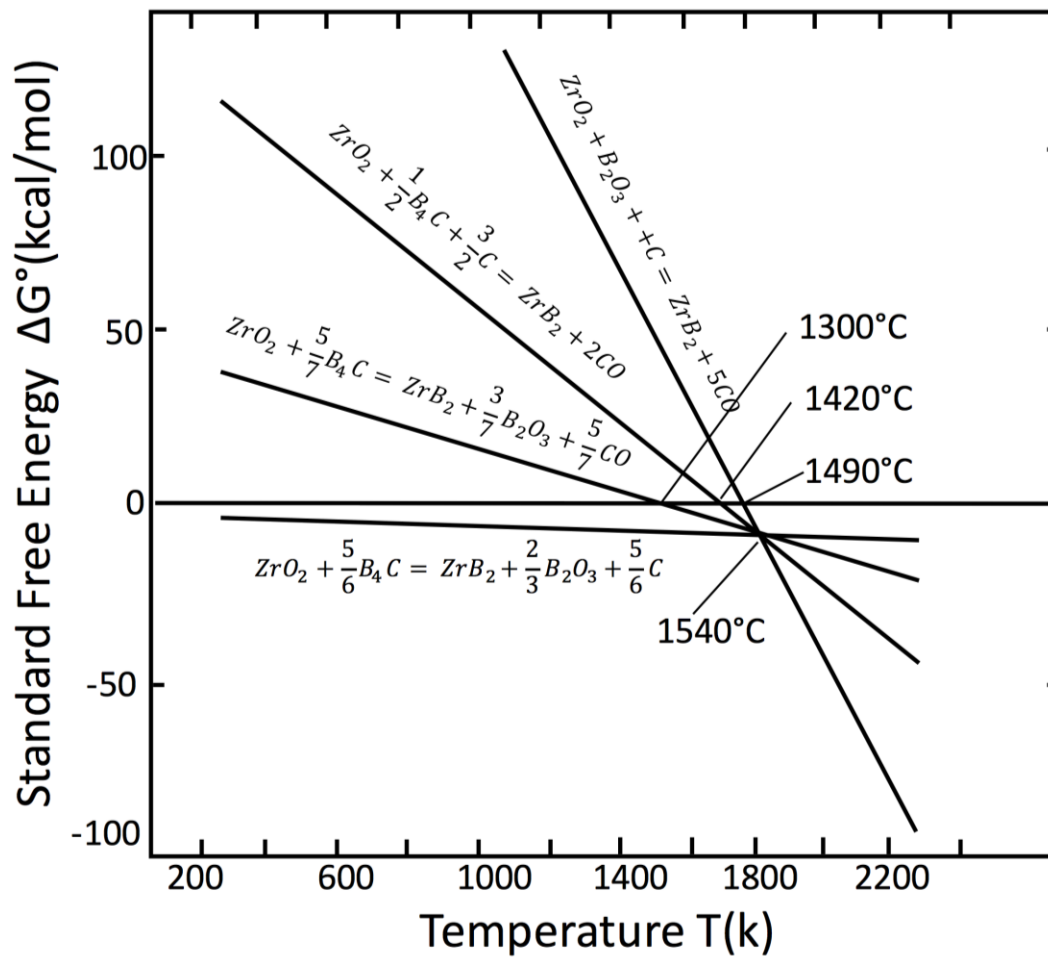


Figure 1

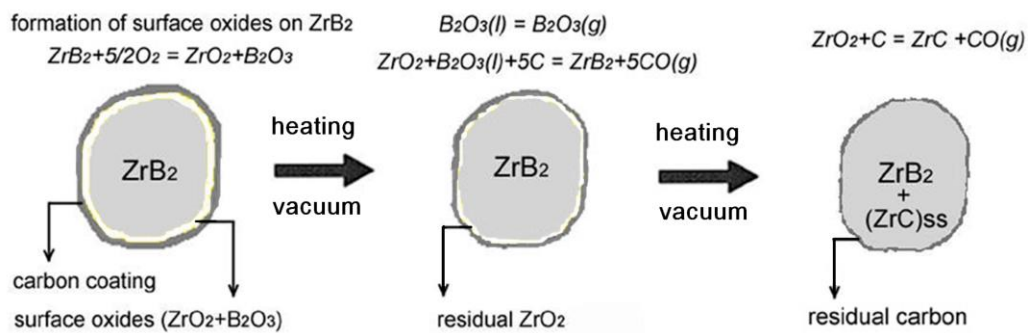


Figure 2

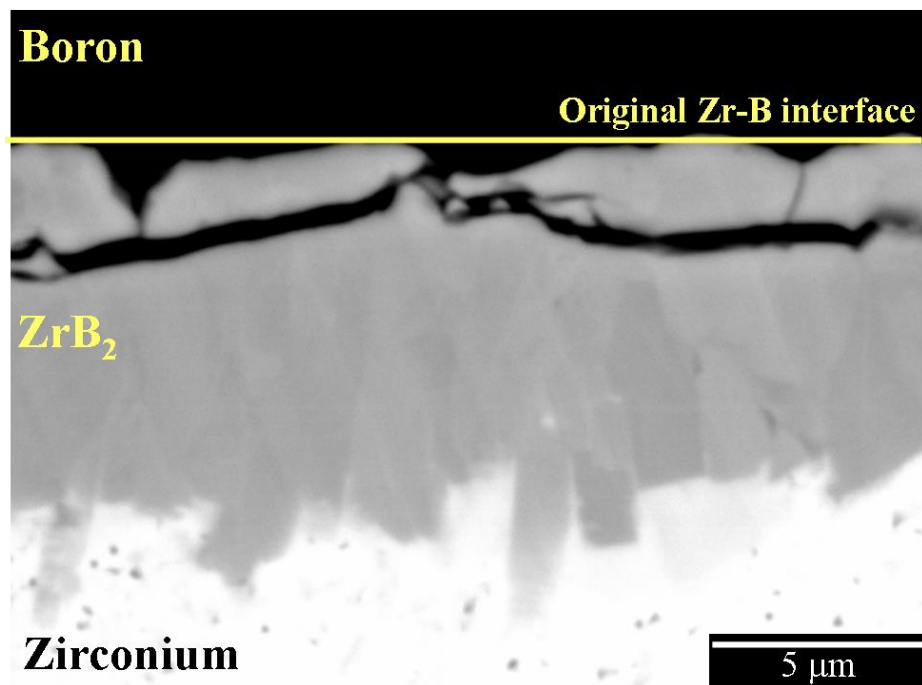


Figure 3

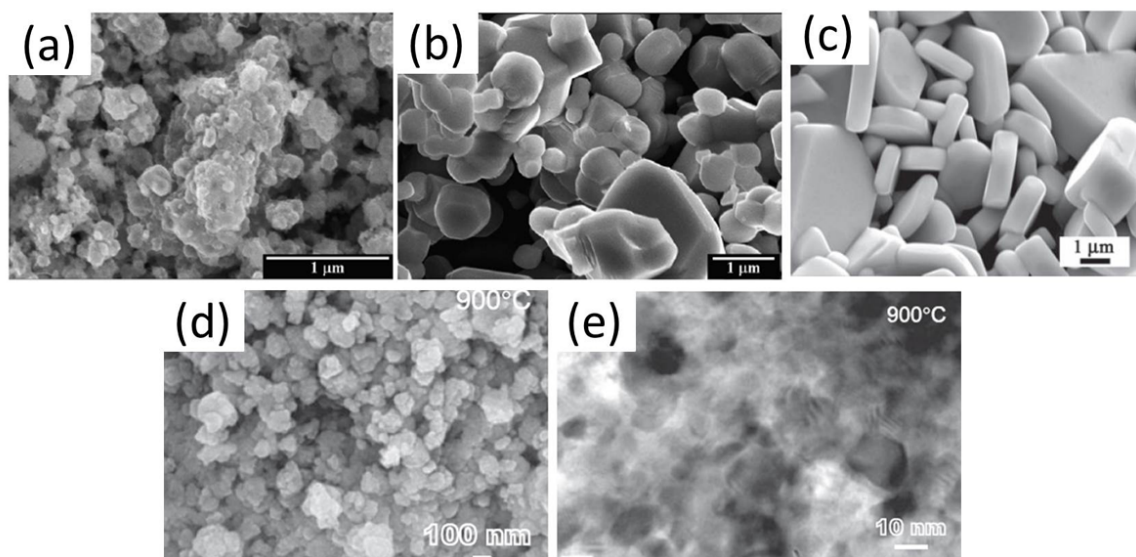


Figure 4

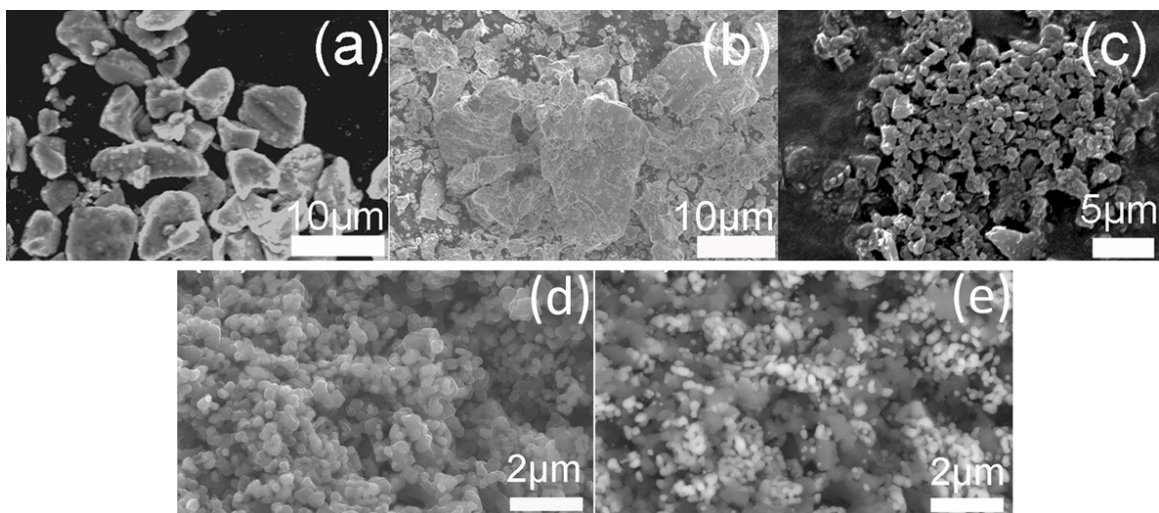


Figure 5

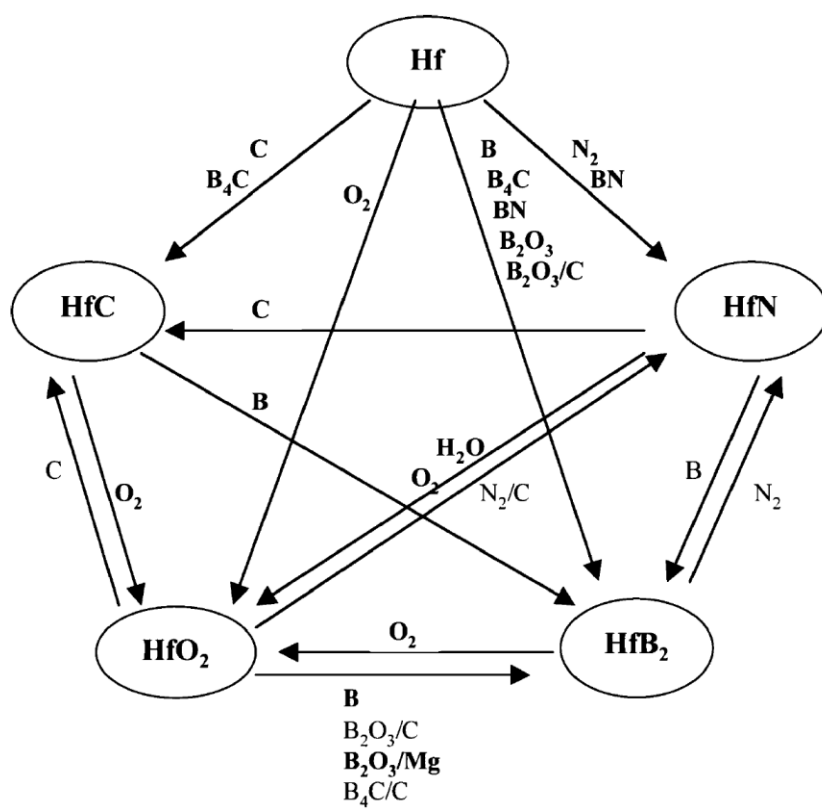


Figure 6

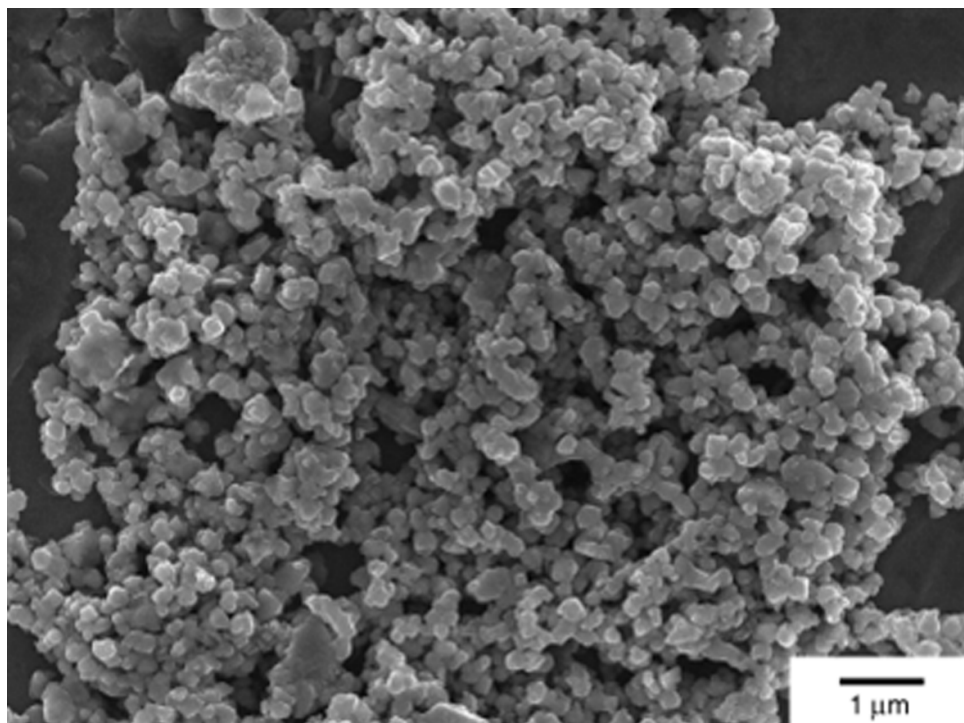


Figure 7

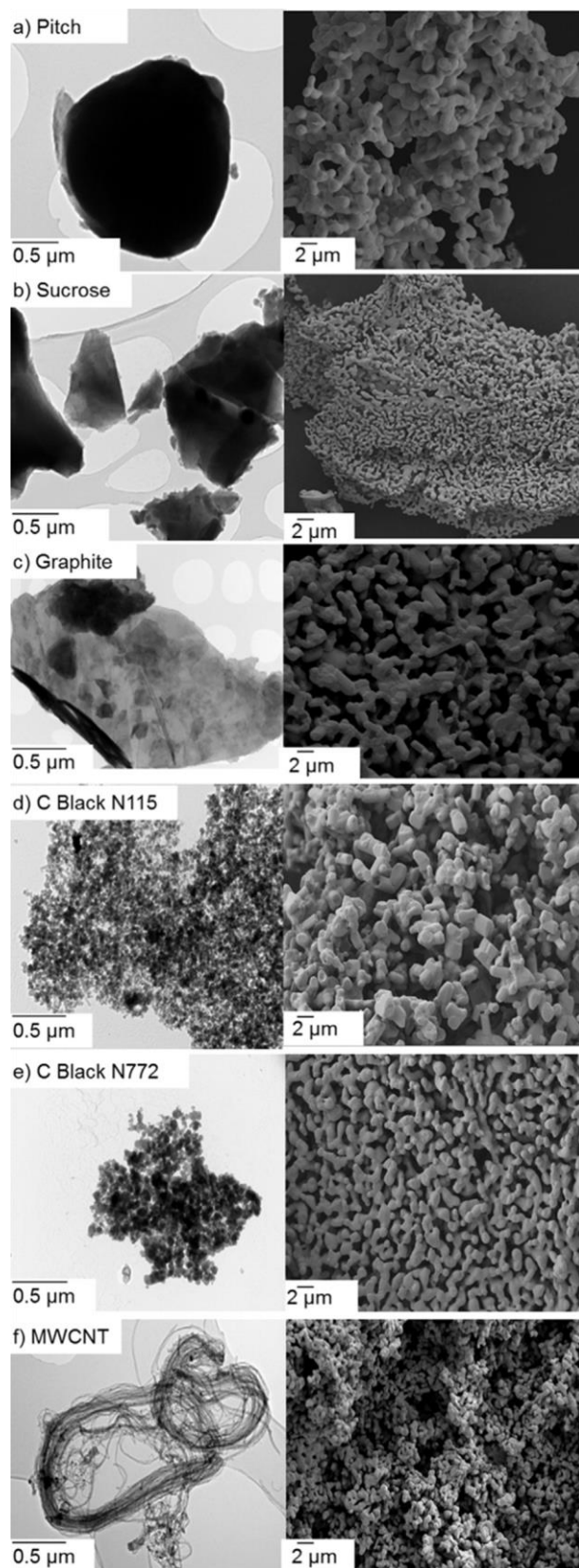


Figure 8